Economic Geology

BULLETIN OF THE SOCIETY OF ECONOMIC GEOLOGISTS

VOL. 113 November NO. 7

Controls on Metal Distributions at the Lisheen and Silvermines Deposits: Insights into Fluid Flow Pathways in Irish-Type Zn-Pb Deposits

Koen Torremans,† Roisin Kyne, Robert Doyle, John F. Güven, and John J. Walsh

Irish Centre for Research in Applied Geosciences, School of Earth Sciences, University College Dublin, Belfield, Dublin, Ireland

Abstract

The world-class Irish Zn-Pb(-Ag) deposits occur within one of the world's major metallogenic provinces. While it has been well documented that these orebodies are structurally controlled, exactly how fluids migrated from source to trap is still poorly understood. Using 3-D modeling techniques, the current study investigates metal distribution patterns at the Silvermines and Lisheen deposits to gain insights into fluid pathways and structural controls on mineralization. Distinct points along segmented normal faults are identified as the feeders to individual orebodies, allowing hot, hydrothermal, metal-bearing fluids to enter host rocks and form orebodies. These points are characterized by highly localized and elevated Ag, Cu, Co, Ni, and As concentrations as well as low Zn/Pb ratios, which increase away from the feeders. Metal distributions are initially controlled by major and minor normal faults and subsequently affected by later oblique-slip dextral and strike-slip faults. High-tonnage areas without typical feeder signals are interpreted to be structural trap sites, which are distal to fault-controlled feeder points. This study highlights both the importance of a well-connected plumbing system for metal-bearing fluids to reach their basinal traps and the control that an evolving structural framework has on spatial distribution of metals.

Introduction

The Irish ore field hosts over 25 economic and subeconomic Zn-Pb deposits including Navan, Lisheen, Galmoy, Tynagh, and Silvermines, containing >20 million metric tonnes (Mt) of Zn + Pb metal (Fig. 1). Zn-Pb mineralization is hosted in the Lower Carboniferous transgressive marine carbonate sequence of limestones, marls, and shales overlying the terrestrial sandstones, conglomerates, and siltstones of the Old Red Sandstone (Philcox, 1984). The Old Red Sandstone unconformably overlies a lower Paleozoic succession of muddy sandstones, siltstones, shales, and volcanic rocks. Most of the ore in the Irish Zn-Pb orefield is lithostratigraphically restricted to the Meath Formation (Pale Beds) of the Navan Group or the Waulsortian limestones and is strongly structurally controlled (Fig. 2; Hitzman and Large, 1986; Philips and Sevastopulo, 1986; Hitzman and Beaty, 1996; Ashton et al., 2015). The Waulsortian-hosted deposits occur in the hanging-wall rocks of complexly segmented normal fault zones that were developed during a Lower Carboniferous rifting event (Hitzman, 1999; Carboni et al., 2003; Bonson et al., 2012). These faults are highly laterally discontinuous, creating horst and graben structures, which control lateral facies variations within the basins (Hitzman and Beaty, 1996). The segmented fault arrays themselves consist of two or more fault segments whose aggregate displacements often constitute a single, kinematically coherent system, with a transfer of displacements between individual segments across accommodation structures known as relay ramps (e.g., Walsh and Watterson, 1988; Childs et al., 1995; Walsh et al., 1999; Fossen and Rotevatn, 2016).

Mineralization within Irish-type Zn-Pb deposits occurs by replacement of Lower Carboniferous marine carbonates as a result of fluid mixing of high-temperature, high-salinity, reducing metal-bearing fluids and low-temperature, medium-salinity seawater-derived fluids (Banks et al., 2002; Wilkinson et al., 2005a, 2009; Barrie et al., 2009; Wilkinson, 2010). Detailed fluid inclusion studies of mineralized veins in lower Paleozoic basement (Everett et al., 1999; Gleeson and Yardley, 2002) and isotope, halogen, and ionic composition of mineralizing fluids (Banks et al., 2002; Kinnaird et al., 2002; Wilkinson et al., 2005a; Walshaw et al., 2006) indicate that fluids derived from evaporated seawater interacted with, and circulated deep within, a highly fractured basement. Migration of (evaporated) seawater brines into basement rocks and later upwelling of ore-bearing fluids during extensional periods has been recognized in carbonate-hosted Zn-Pb deposits throughout Europe (see review in Muchez et al., 2005). Based on textural, isotopic, and geochemical signatures of layered sphalerite at Galmoy and Navan, the fundamental trigger for rapid sphalerite precipitation at these deposits is interpreted

† Corresponding author: e-mail, koen.torremans@icrag-centre.org

© 2018 Gold Open Access: this paper is published under the terms of the CC-BY license.

©2018 Society of Economic Geologists; *Economic Geology*, v. 113, no. 7, pp. 1455–1477
ISSN 0361-0128; doi: 10.5382/econgeo.2018.4598; 23 p.
Supplementary files available online.

Submitted: April 9, 2018
Accepted: September 5, 2018

Downloaded from https://pubs.geoscienceworld.org/segweb/economicgeology/article-pdf/113/7/1455/4558470/1455-1477.pdf
by Univ College Dublin user

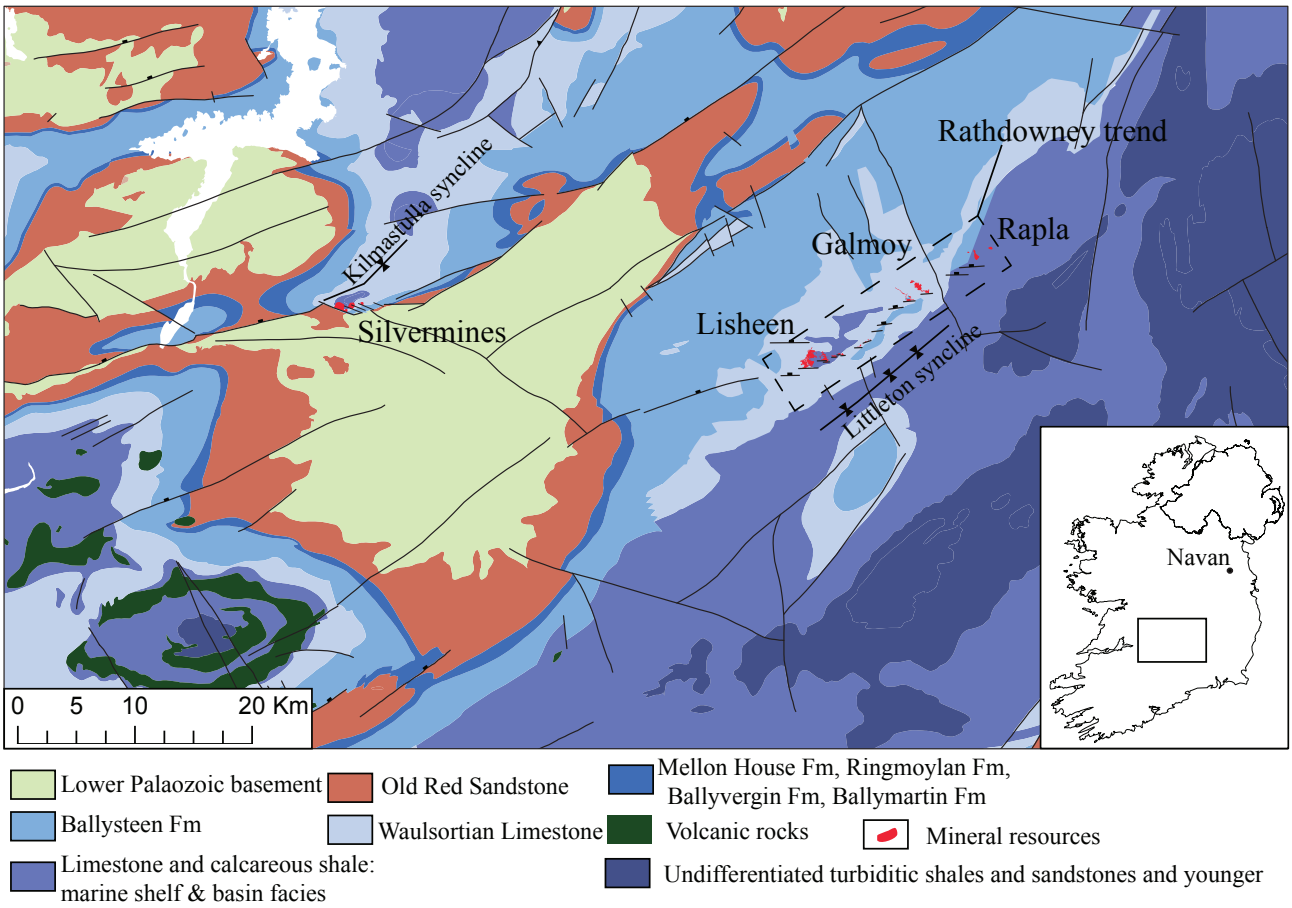

Fig. 1. Geologic map of the study area showing the location of the Lisheen, Silvermines, and Galmoy Zn-Pb mines and the Rapla Zn-Pb prospect. The inset shows the location of this map in Ireland, as well as the position of the Navan Zn-Pb deposit. The geology and faults are modified from the Geological Survey Ireland (2017) as well as from mapping performed by John Colthurst for the Rathdowney trend (pers. commun., 2015). The marine carbonate sequence hosting the Irish-type Zn-Pb ore is shown in shades of blue. Orebodies are indicated in red.

to be the influx of deep sulfur-poor hydrothermal fluids into a shallow reservoir of bacteriogenic sulfur-rich fluids (Barrie et al., 2009; Gagnevin et al., 2012, 2014). Other studies have also interpreted fluid mixing to be a primary precipitation mechanism at Tynagh (Banks and Russell, 1992), Navan (Fallick et al., 2001; Blakeman et al., 2002), Lisheen (Eyre, 1998; Wilkinson et al., 2005b), and Silvermines (Andrew, 1986; Samson and Russell, 1987). Reactive transport simulations performed by a number of authors show that mixing of acidic hydrothermal brines with groundwater or seawater reservoirs in carbonates in the immediate hanging wall or footwall of faults creates zones of contemporaneous carbonate dissolution and sulfide precipitation, as well as precipitation farther away from the faults (Corbella et al., 2004, 2006, 2014; Anderson and Thom, 2008).

The majority of ore-stage fluid inclusions in the Irish ore field show homogenization temperatures of 130° to 240°C (Wilkinson, 2010), and recent clumped C-O isotope analyses on ore-stage carbonates have demonstrated similar temperatures (Hollis et al., 2016). Under these temperatures, and taking into account the end-member compositions of the two mixing fluids, the mobility of Zn and Pb is mainly sensitive to changes in pH, T, and f_{O_2}, with Zn generally being more mobile than Pb (Anderson, 1975; Barnes, 1979, 1983; Sverjensky, 1986; Anderson and Garven, 1987; Cooke et al., 2000). Such differences in metal mobility can lead to deposit-scale metal zonation. Where structurally controlled, these zonations can emanate from feeders where metal-bearing fluids enter the site of mineralization.

This study addresses in detail how the structural and stratigraphic framework controls fluid pathways and metal distributions within Irish-type Zn-Pb deposits and is of importance for both mineral exploration and mining. We examine local controls on mineralization and the locations of feeder zones and track fluid pathways along faults and through host rocks from proximal to distal areas within two Irish-type deposits, Lisheen and Silvermines. This research builds upon previous work on metal distributions that shows the existence of metal zonation and feeders in Irish-type Zn-Pb deposits (Andrew, 1986; Blakeman et al., 2002; Lowther et al., 2003; Fusciardi et al., 2004; Davidheiser-Kroll et al., 2013; Ashton et al., 2015). For example, feeder zones at Lisheen and Silvermines were interpreted based on the association of low Zn/Pb ratios with textural and mineralogical evidence, such as the presence of tennantite, boulangerite, guitermanite, and chalcopyrite in the near hanging wall or along faults (Taylor, 1984; Fusciardi et al., 2004). Metal distribution patterns at the Navan

Downloaded from https://pubs.geoscienceworld.org/segweb/economicgeology/article-pdf/113/7/1455/4558470/1455-1477.pdf
by Univ College Dublin user

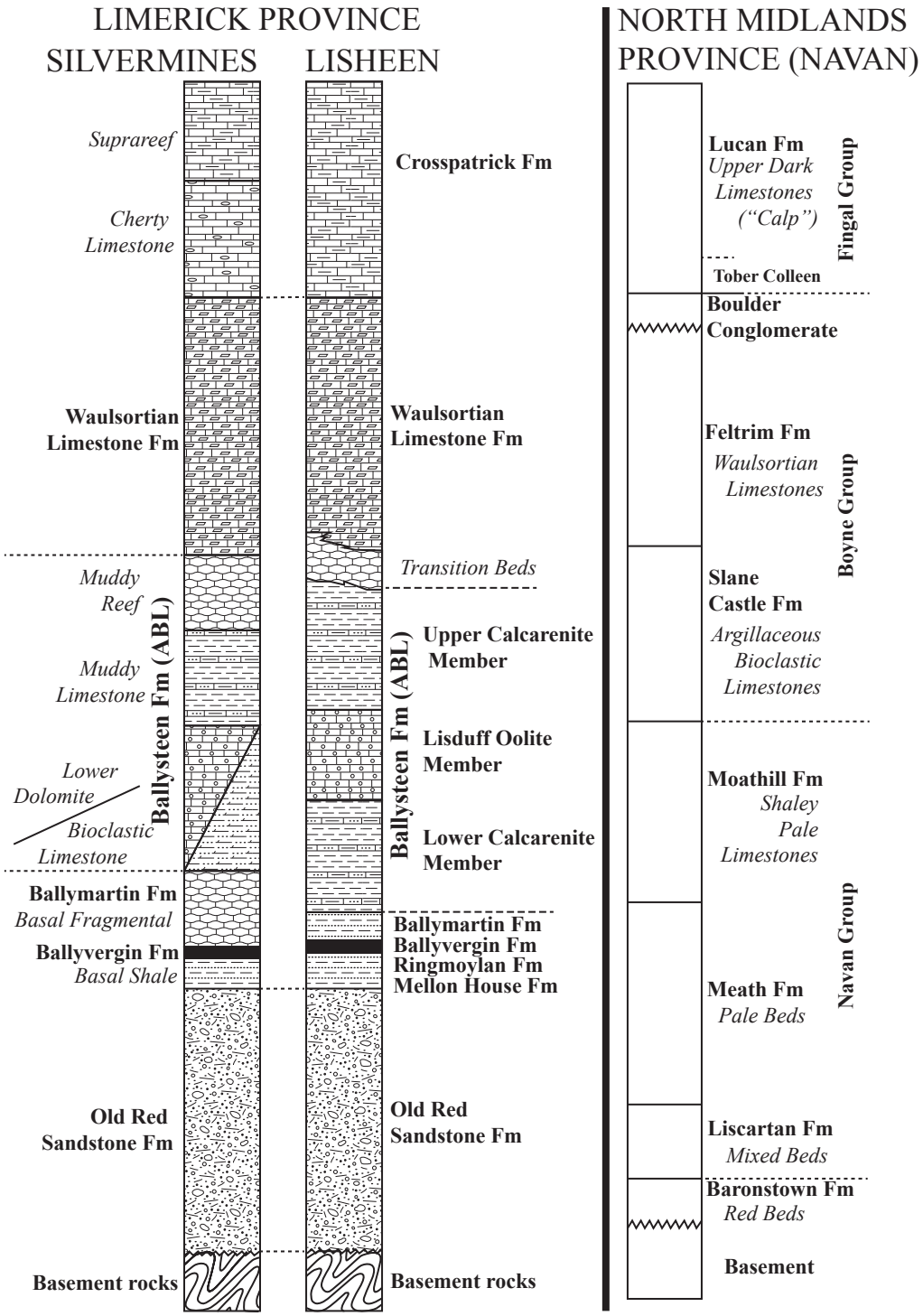

Fig. 2. Stratigraphic columns for the units above the basement unconformity for the Limerick province (Silvermines and Lisheen) and the North Midlands province (e.g., Navan). These lithostratigraphic provinces are based on the work of Philcox (1984) and Sevastopulo and Wyse-Jackson (2009). Local names are given in italics and established stratigraphic names in bold. The stratigraphy of Silvermines is based on Taylor and Andrew (1978), Philcox (1984), and Andrew (1986); that of Lisheen is from Shearley et al. (1996) and Hitzman et al. (2002); Navan stratigraphy is derived from Philcox (1984), Strogen et al. (1990), and Ashton et al. (2015). Abbreviation: ABL = argillaceous bioclastic limestones.

deposit are complex, and the deposit is strongly complicated by fault scarp degradation through low-angle tectonic slides. Nevertheless, based on sulfur isotope values and high Zn + Pb enrichments along faults, several feeder zones have been identified in the Main orebody of the Navan deposit (Blakeman et al., 2002; Davidheiser-Kroll, 2014; Ashton et al., 2015).

As a prelude to our detailed analysis of each deposit, we first outline the basic 3-D modeling approach and the data used

Downloaded from https://pubs.geoscienceworld.org/segweb/economicgeology/article-pdf/113/7/1455/4558470/1455-1477.pdf
by Univ College Dublin user

in this study. This is followed by descriptions of the structural framework of each deposit, as defined from the 3-D geologic modeling, a brief overview of the associated ore mineral paragenesis, and a comparison of the metal distributions with their paragenetic, lithostratigraphic, and structural frameworks. We conclude with a discussion of some of the principal technical issues associated with structurally controlled mineralization in the Irish ore field, followed by a consideration of implications for future exploration and mining.

Methodology

The structural framework and stratigraphy at the Silvermines and Lisheen deposits was investigated using proprietary 3-D geomodeling software packages. Vulcan (Maptek) was used for explicit picking of detailed fault and horizon geometries in areas of high data density and structural complexity. The explicitly picked horizons and faults from Vulcan were then used as direct input into SKUA-GoCAD (Paradigm) and Mining Suite plugins of Mira Geoscience. Here, interpolations of several horizons and fault points were carried out using the discrete smooth interpolator (e.g., Caumon et al., 2009). Data validation, exploration, and visualization were carried out with Leapfrog3DGeo (ARANZ Geo Ltd.). Additional data entry, data validation, and georeferencing was accomplished using MOVE (Midland Valley Ltd.), ArcMap (ESRI), and QGIS (qgis.org, FOSS). In order to understand the interplay between the structural and stratigraphic architecture within the two deposits, unit juxtapositions along the faults were analyzed using Allan maps (Allan, 1989).

Structure and horizon model interpretations are based on a variety of data sources. The data set for Silvermines consists of legacy data that were digitized and georeferenced for this study. These legacy data include paper drill core logs, assays (Pb, Zn, and sparse Ag), mine plans with geology and structures, and geologic sections based on drill hole and underground information as well as surface geologic maps from the Geological Survey Ireland and published literature (e.g., Taylor, 1984; Andrew, 1986; Lee and Wilkinson, 2002; Reed and Wallace, 2004). For the Lisheen deposit, all data were available digitally, including a full surface and underground drill hole database, core photos, an extensive suite of assay data, detailed 3-D digitized face mapping at 4-m horizontal intervals along development drives of the entire mine, and surface geologic maps. This study has built upon earlier Vulcan models that were developed when the mine was in operation.

At Lisheen, analytical data is available for a large suite of metals as well as a large specific gravity (density) data set. Elemental concentrations of Zn, Pb, Fe, Cu, Ni, Ag, Co, As, S, Tl, and Sb were measured by ALS Loughrea over the period of mine operation using oxidizing aqua regia digestion inductively coupled plasma-optical emission spectrometry (ICP-OES). Atomic absorption spectrometry (AAS) was used for samples over upper calibration limits. Metal distribution maps were generated in Vulcan using estimated grades and tonnages from a geostatistics-based resource block model that incorporated >70,000 1-m-composited assays. The data in the block model are length-by-density–weighted grades and are displayed in maps as the total tonnage of a specific metal contained within a 4- × 4-m vertical column through the orebody. In the Zn/Pb ratio map, columns with <3 t of lead are not shown in order to remove anomalously high or low ratio values resulting from trace Zn and Pb grades.

At Silvermines, systematic assay analyses for Pb and Zn were carried out, whereas Ag was assayed only in certain areas of the mine. Specific gravity (density) and Fe analytical data were not available, therefore metal distributions were determined using length-weighted average grades (as opposed to length-by-density–weighted grades at Lisheen). Some 22,200 assays that included Zn and Pb grades were composited into 1-m segments, as well as 2,800 Ag assays. A length-weighted composite grade for each metal was then generated for each segment. The ratios were calculated, and the resultant grade or ratio values were inverse distance weighted using a smooth neighborhood-type interpolation with a search radius of 50 m and smoothing factor of one. This search radius was chosen as a trade-off between showing internal variation for the average exploration drill hole spacing in the G zone and B zone (30 m) on the one hand and general trends in areas with lower data density on the other. Points with ≤0.25 ppm Ag and <0.1 wt % Zn or Pb were not used in the interpolations. In the Zn/Pb ratio maps, points with <3 wt % of Zn + Pb are not used to remove anomalously high or low ratio values resulting from trace Zn and Pb grades.

Results and Interpretation—Lisheen Deposit

The Lisheen mine in County Tipperary was mined for 17 years, from 1999 until December 2015. It produced 22.4 Mt at 11.63 wt % Zn and 1.96 wt % Pb. Mineralization at Lisheen consists of several, largely stratiform, massive sulfide bodies at or near the base (generally within 30 m) of the Waulsortian carbonates and breccias. This mineralization is enveloped by semimassive, disseminated, and vein-hosted sulfides. The Lisduff Oolite Member of the Ballysteen Formation is also occasionally mineralized in the footwall of normal faults, as is the top of the Ballysteen Formation (Fusciardi et al., 2004). The deposit comprises six distinct orebodies defined by a cutoff of 40 wt % combined Zn + Pb + Fe (Fig. 3). These orebodies are referred to as Main zone, Derryville, Island zone, and Bog zone west, central, and east.

Key structural and stratigraphic observations

The Lisheen deposit is located on the southern limb of the Littleton regional syncline. Several families of structures are identified at Lisheen (Fig. 3):

1. Firstly, the most important structure is an array of E-ENE–trending left-stepping normal fault segments (bold red lines in Fig. 3). These faults are components of the Rathdowney trend, a regional ENE-trending fault system (Fig. 1). Similar normal faults identified within the Galmoy and Rapla orebodies are also components of the Rathdowney trend (Hitzman, 1999). Five major fault segments define the southern end of individual Waulsortian-hosted orebodies at Lisheen (Fig. 3). These fault segments, from west to east, are Main zone west, Main zone east, Derryville, and Bog zone west and east. Normal fault displacements are on the order of 160 to 220 m, with NW-dipping relay ramps transferring the displacement from one segment to another. The Killoran fault zone was originally a breaching normal fault, which was later reactivated, between normal

Downloaded from https://pubs.geoscienceworld.org/segweb/economicgeology/article-pdf/113/7/1455/4558470/1455-1477.pdf
by Univ College Dublin user

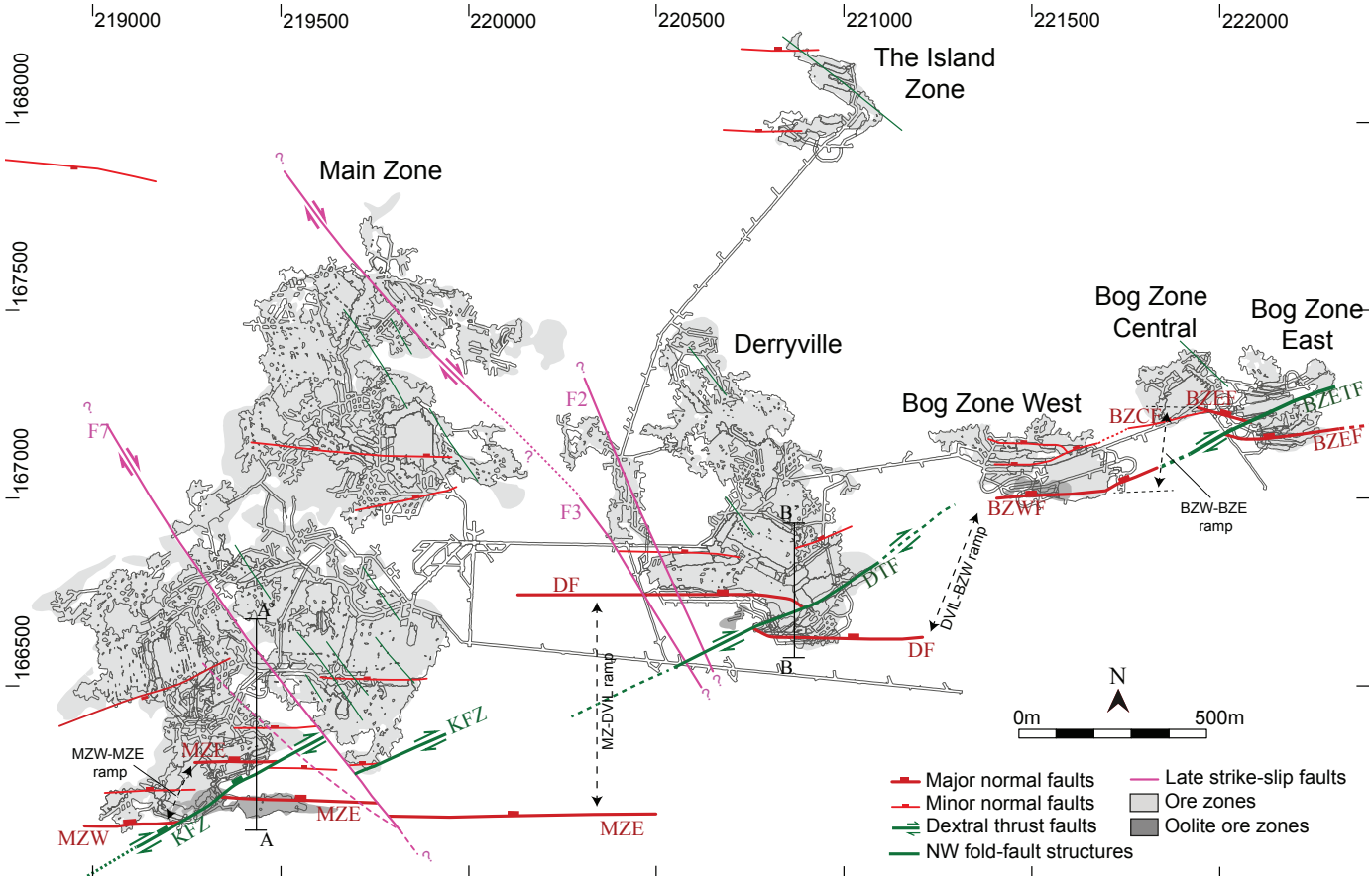

Fig. 3. Plan view of Lisheen with the main structures and orebodies at a cutoff of 40 wt % Zn-Pb + Fe resource. Grid references are relative to the Irish Grid TM65 datum. Lines A-A' and B-B' refer to the position of cross sections in Figure 6. Abbreviations: BZCF = Bog zone central fault, BZEF = Bog zone east fault, BZETF = Bog zone east transpressive fault, BZWF = Bog zone west fault, DF = Derryville fault, DTF = Derryville transpressive fault, KFZ = Killoran fault zone, MZ-DVIL = Main zone-Derryville, MZE = Main zone east fault, MZW = Main zone west fault.

fault segments Main zone east and Main zone west (Kyne et al., 2017). Similarly, the Bog zone east transpressive fault is interpreted as a reactivation of what was originally a footwall-breaching fault between Bog zone west and Bog zone east. The Bog zone central fault represents a suite of hanging-wall breaching faults of the relay ramp zone between the Bog zone east and west faults. Many minor normal faults occur with displacements of up to 15 m and strikes parallel to the major normal faults.

2. Secondly, low-displacement (<10 m) NW-trending normal faults, monoclines, and fault-bend folds are observed throughout the various orebodies. Some of these structures have been mapped and are shown in Fig. 3, although many more remain to be constrained.
3. Thirdly, NE-trending dextral oblique-slip reverse faults crosscut the segmented normal faults (Fig. 3). The Derryville and Bog zone east transpressive faults have vertical and horizontal displacements of 92 to 123 m and 45 m, respectively. The east-west to northeast normal faults are often reactivated, sometimes significantly reducing the observed normal throw. In the Main zone, the NE-trending Killoran-breaching normal fault has been reactivated as a dextral oblique slip transpression fault, also confirmed by kinematic indicators (Fusciardi et al., 2004). Several fault-bend folds and occasional overfolds of the Ballysteen Formation occur in the hanging wall of the normal faults. These folds are predominantly east-west to east-west-northeast trending—that is, parallel to the EW– to EW-NE–trending normal fault segments. All these structures are interpreted to have formed in a transpressive regime during N-S–oriented shortening during the Variscan orogeny (Coller, 1984; Hitzman, 1999).
4. Finally, predominantly dextral NW-trending, subvertical strike-slip faults crosscut all previous structures. Displacements vary significantly, up to a maximum of 75 m of strike-slip movement on the F7 fault (Fig. 3). These post-Variscan faults are associated with higher rates of groundwater flow and are interpreted to be post-Variscan in age. Similar structures in Northern Ireland have been attributed to north-south Alpine compression within either the Paleocene or the Oligocene (Carboni et al., 2003; Fusciardi et al., 2004; Cooper et al., 2012).

Mineralization

A generalized paragenesis of the Lisheen deposit is shown in Figure 4. This summary paragenesis is based on recent detailed observations (including Doran et al., 2017; Turner and McClenaghan, 2017) and on a review of a number of

Downloaded from https://pubs.geoscienceworld.org/segweb/economicgeology/article-pdf/113/7/1455/4558470/1455-1477.pdf
by Univ College Dublin user

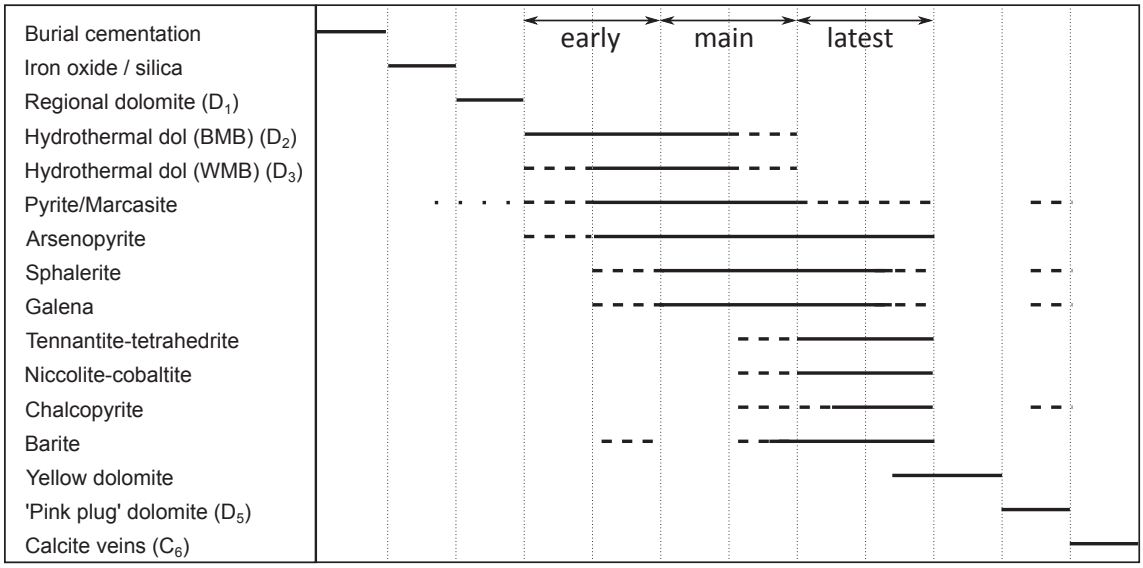

Fig. 4. Generalized paragenesis at Lisheen based on new observations and a number of previous studies (Shearley et al., 1996; Redmond, 1997; Eyre, 1998; Stewart, 1999; S. Strashimirov, unpub. report, 1999; Cruise, 2000; Hitzman et al., 2002; Wilkinson et al., 2005b). To provide a link with the literature, the annotations D_1 D_2, D_3, D_5, D_6, and C_6 refer to the carbonate classification of of Wilkinson et al. (2005b). The BMB and WMB are black matrix breccia and white matrix breccia, respectively, and refer to broad categories of types of replacive hydrothermal dolomite in the breccias.

previous studies (Shearley et al., 1996; Redmond, 1997; Eyre, 1998; Stewart, 1999; S. Strashimirov, unpub. report, 1999; Cruise, 2000; Hitzman et al., 2002; Wilkinson et al., 2005b). The Waulsortian limestone was regionally dolomitized before any sulfide mineralization, and minor dolomitization occurs in nonargillaceous beds of the overlying Crosspatrick Formation (Sevastopulo and Redmond, 1999). This regional dolomitization extends across the southeastern end of the Rathdowney trend (Shearley et al., 1996; Hitzman et al., 1998; Sevastopulo and Redmond, 1999; Wilkinson et al., 2005a). Broadly, three stages of sulfide mineralization can be recognized, with an early, main, and latest stage, although it is best to consider these stages as a gradually evolving system. The earliest sulfide mineralization is dominated by Fe sulfides, currently forming much of the pyrite cap to Zn-Pb orebodies seen throughout the deposit. These disseminated to massive Fe sulfides (pyrite, marcasite) show highly fractionated δ^{34}S signatures interpreted to be the result of bacteriogenic sulfate reduction (–38 to –44‰; Hitzman et al., 2002; Wilkinson et al., 2005b). Minor non- to weakly colloform pink-brown sphalerite and galena with similar bacteriogenic signatures precipitated with these early Fe sulfides, infilling intergranular dolomite porosity (Hitzman et al., 2002; Wilkinson et al., 2005b). Multiple stages of early pyrite are identified, typically with colloform pyrite/marcasite followed by more coarse-grained varieties associated with the minor early-stage sphalerite and galena (Fusciardi et al., 2004; Wilkinson et al., 2005b). Bravoite rims on early pyrite are interpreted to represent a change from predominantly Fe sulfides to Zn-Pb sulfides concomitant with the more pronounced influx of hot Zn-Pb metal-bearing hydrothermal fluids into the host rocks (Eyre, 1998; Fusciardi et al., 2004; Wilkinson et al., 2005b, 2011).

The main Zn-Pb sulfide stage occurs as predominantly sphalerite and galena, progressively replacing and overprinting breccia matrix dolomite, clasts of regional dolomite, and early Fe sulfides (Hitzman et al., 2002). This mineralization stage is characterized by a polymetallic sulfide assemblage of predominantly sphalerite, galena, pyrite, and minor marcasite and, locally, niccolite, arsenopyrite, chalcopyrite, tennantite-tetrahedrite, and barite (Redmond, 1997; Sevastopulo and Redmond, 1999; S. Strashimirov, unpub. report, 1999; Hitzman et al., 2002). Multiple stages are seen within the main Zn-Pb sulfide stage, characterized by complex replacement and overprinting relationships. Broadly speaking, the main Zn-Pb sulfide stage can be subdivided into a main stage of predominantly sphalerite, galena, and Fe sulfides and a latest stage, with increasing addition of niccolite, chalcopyrite, tennantite-tetrahedrite, and barite. Main ore-stage sulfides have higher δ^{34}S (mode at –10‰), and the latest ore-stage sulfides have the highest δ^{34}S values (–3.0 ± 8.5‰, 1σ), interpreted to be the result of thermal sulfate reduction at increasingly higher temperatures (Eyre, 1998; Wilkinson et al., 2005b). Niccolite and bravoite are the main Ni-bearing phases, but Ni also occurs as a trace element in other minerals such as pyrite and sphalerite (Wilkinson et al., 2005b, 2011). Copper occurs mainly in chalcopyrite and tennantite, in accessory bornite, or as a trace element in Cu-bearing sphalerite. Silver occurs in solid solution in tennantite-tetrahedrite, galena, and sphalerite (Wilkinson et al., 2005b). Arsenic is mainly hosted in arsenian pyrite, tennantite, and arsenopyrite, and Ba is found in barite and barian feldspar (Hitzman et al., 2002; Wilkinson et al., 2005b).

Metal distributions at Lisheen

Figure 5 shows metal tonnage distribution maps of Zn, Pb, Fe, Cu, Ni, As, Cd, and Ag as well as the Zn/Pb, Zn/Fe, Fe/(Zn + Pb), and Zn/Cd ratios in relation to the structural framework as interpreted by 3-D modeling. Each point on Figure 5 represents the estimated total tonnage of a specific metal

Downloaded from https://pubs.geoscienceworld.org/segweb/economicgeology/article-pdf/113/7/1455/4558470/1455-1477.pdf
by Univ College Dublin user

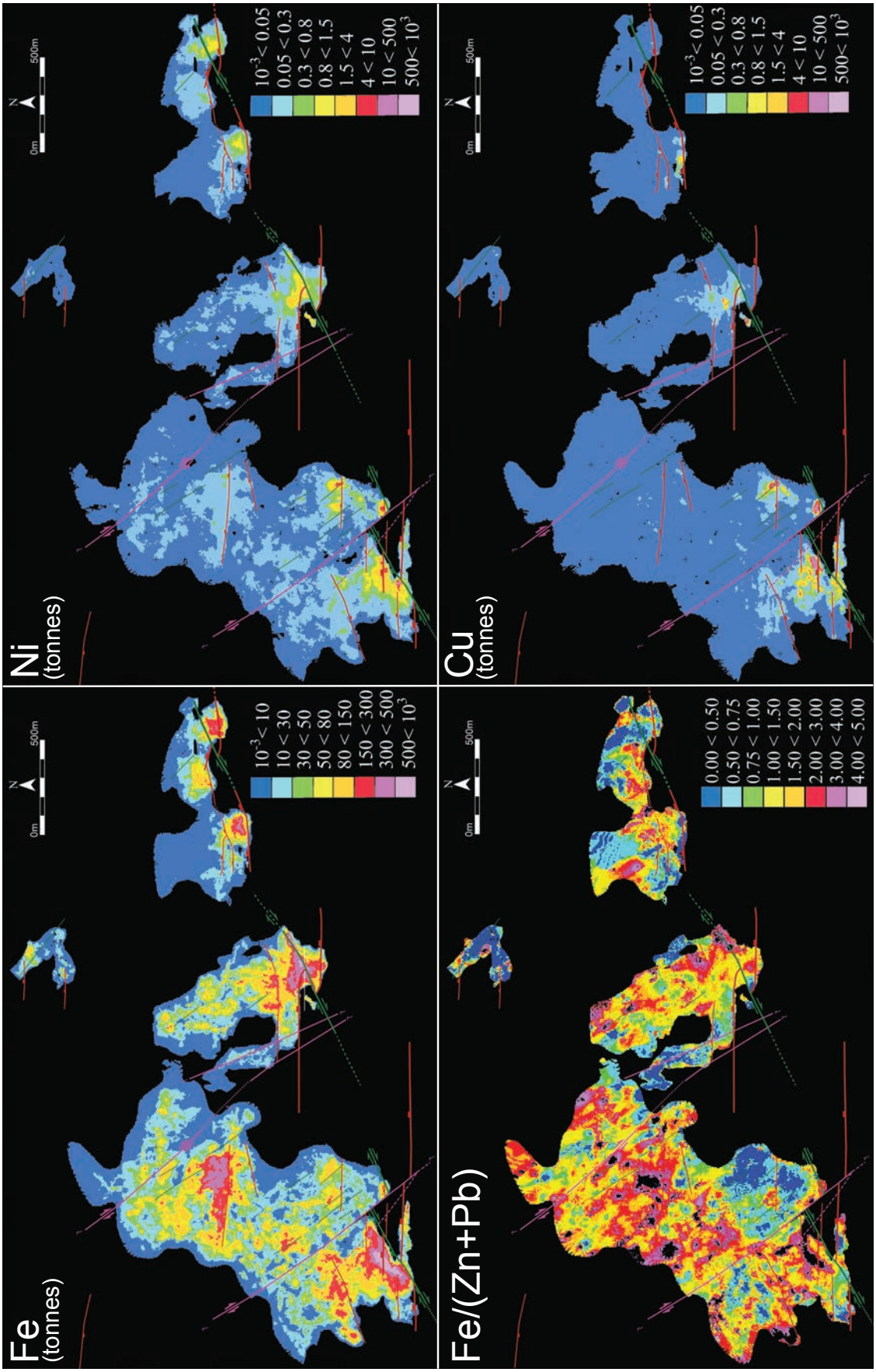

Fig. 5. Metal tonnage distribution maps of Fe, Ni, Cu, Zn, Pb, Ag, Cd, and As as well as Zn/Pb, Zn/Fe, Zn/Cd, and Fe/(Zn + Pb) ratios at the Lisheen deposit in relation to the main structural framework. Refer to text for explanation of trends and relationships. Tonnages are displayed as the total tonnage of a specific metal contained within a 4- × 4-m vertical column through the orebody, as defined from the block model (see methodology section for more details). Legends are in tonnes of the given element or ratios in the case of Zn/Pb, Zn/Fe, Zn/Cd, and Fe/(Zn + Pb). Structures are colored in the same way as Figure 3, with normal faults (red), dextral oblique-slip thrust faults (green), northwest fold-fault structures (dark green), and late strike-slip faults (magenta).

Downloaded from https://pubs.geoscienceworld.org/segweb/economicgeology/article-pdf/113/7/1455/4558470/1455-1477.pdf
by Univ College Dublin user

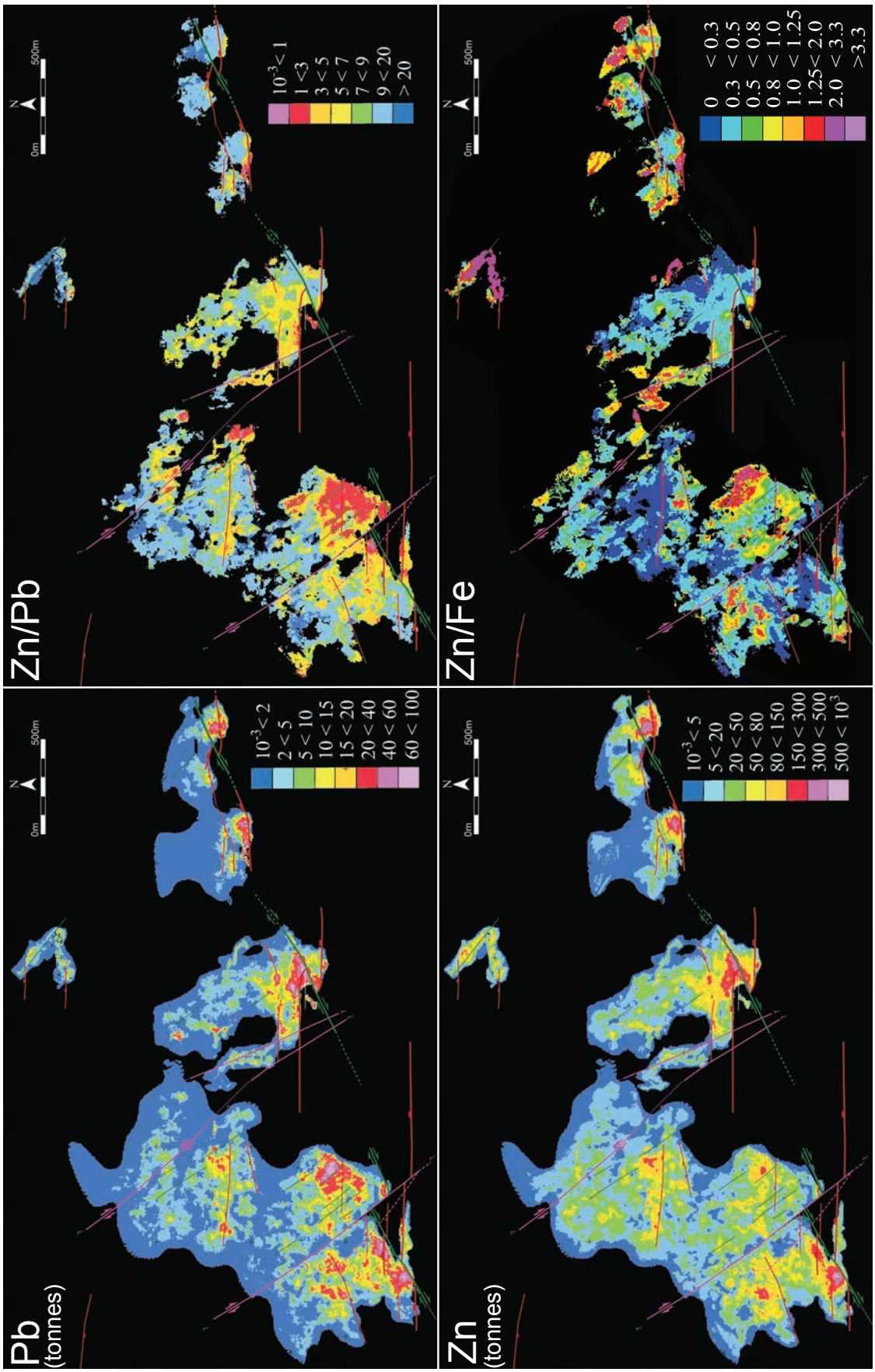

Fig. 5. *(Cont.)*

Downloaded from https://pubs.geoscienceworld.org/segweb/economicgeology/article-pdf/113/7/1455/4558470/1455-1477.pdf
by Univ College Dublin user

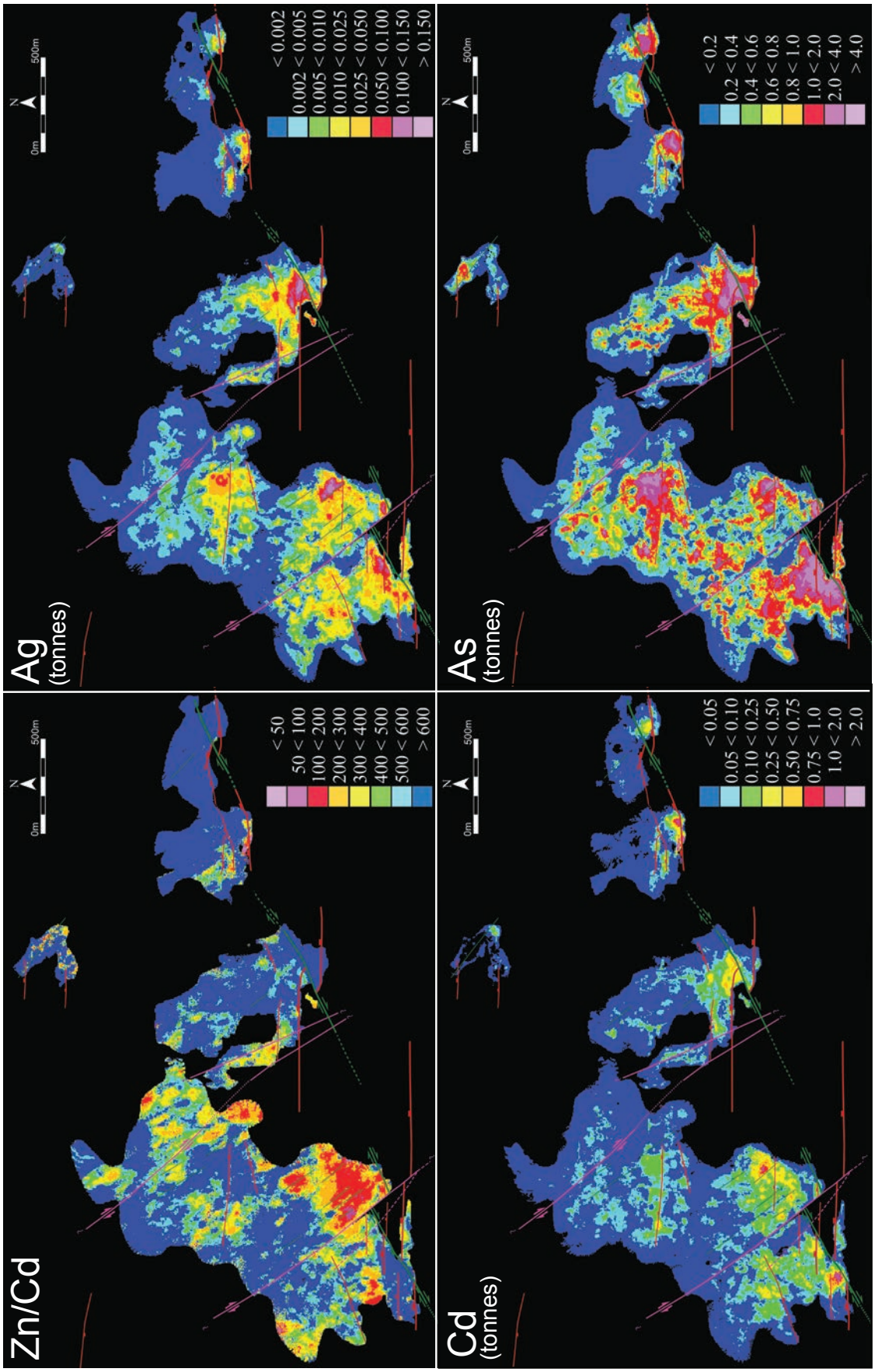

Fig. 5. *(Cont.)*

Downloaded from https://pubs.geoscienceworld.org/segweb/economicgeology/article-pdf/113/7/1455/4558470/1455-1477.pdf
by Univ College Dublin user

contained in a 4- × 4-m vertical column through the orebody block model (see methodology section for more details). Figure 6 shows two NS-oriented cross sections through the Main and Derryville zones and several tonnage slices through the block model.

High Fe tonnages occur in the hanging-wall rocks of both major and minor normal faults (Fig. 5). These faults also control the distribution of the thick pyrite caps that sit above the Zn-Pb mineralization in the hanging-wall rocks of these faults (e.g., Fig. 6E, K).

Cu, Ni, Co, Cd, and Ag show high tonnages proximal to distinct points (which are interpreted as feeders) along the major normal fault segments (Killoran fault zone, Main zone east fault, Derryville fault, Bog zone west fault, Bog zone east fault), with tonnages of these metals decreasing with distance from the interpreted feeder faults (Figs. 5, 6G, H, M, N). This decrease in metal tonnages occurs over quite a small distance, on the order of 10 to 100 m. These high Cu-Ni-Co-Cd-Ag tonnages occur both in the Waulsortian in the hanging wall and in the Lisduff Oolite Member in the footwall of the normal faults. Mineral assemblages at these feeders include tennantite-tetrahedrite, niccolite, cobaltite, chalcopyrite, Ag sulfosalts, and barite in addition to sphalerite, galena, and pyrite (Redmond, 1997; Fusciardi et al., 2004). Orebodies hosted in the Lisduff Oolite Member of the Ballysteen Formation are spatially restricted (darker gray in Fig. 3). When restored to their original position before Variscan dextral oblique-slip movement on reverse faults, these zones

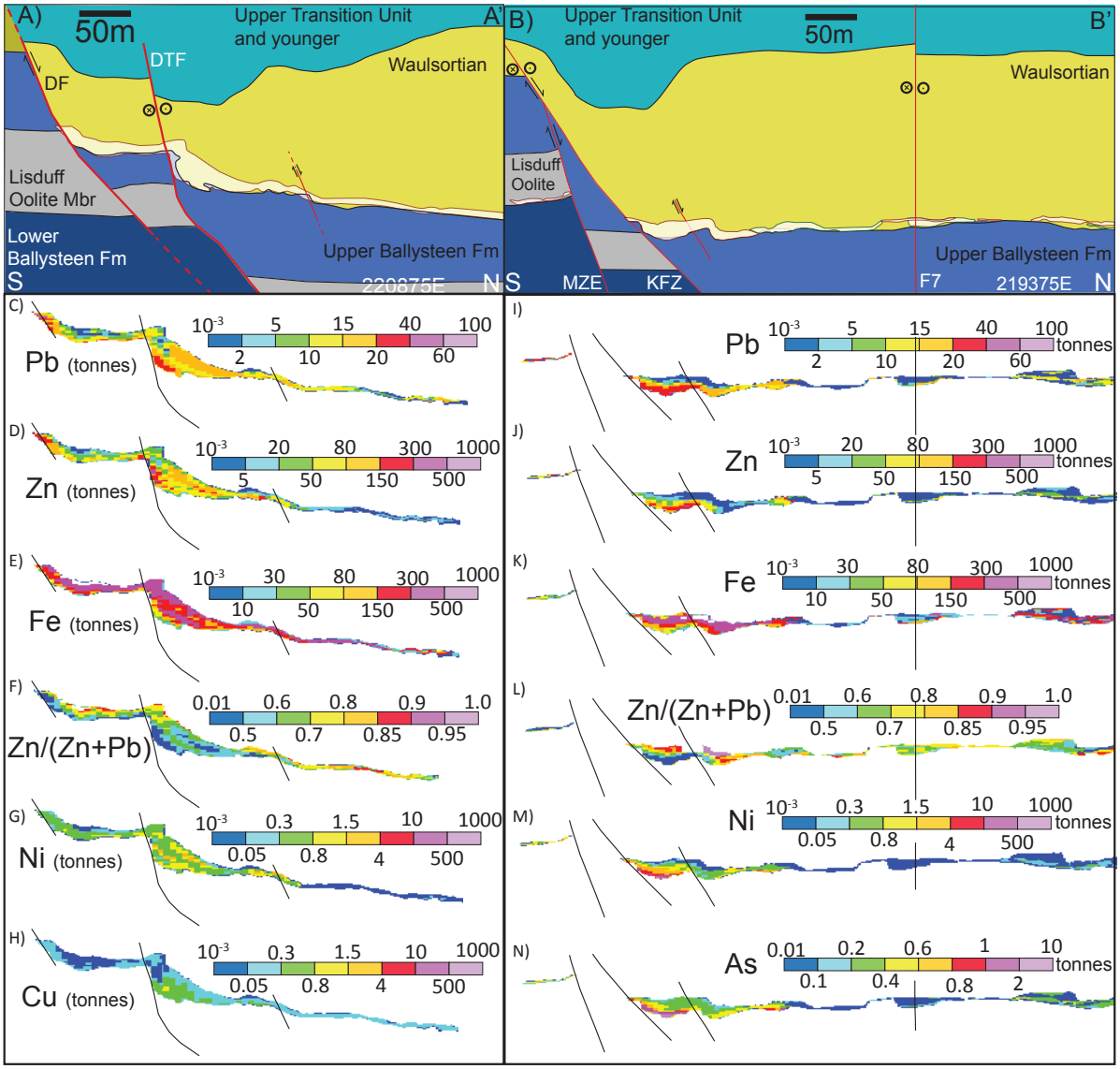

Fig. 6. Representative north-south cross sections at the Lisheen deposit showing structures, base of rock types, and metal tonnages as defined by a block model. The orebodies in (A) and (B) are shown in white outlines, as defined from mine resources in November 2015. Location of the sections is indicated in Figure 3. (A) Section at 220875E (Irish Grid) through the Derryville zone. DF = Derryville normal fault, DTF = Derryville dextral transpressive fault, which is heavily inverted locally with overfolding in places. (B) Section at 219375E (Irish Grid) through Main zone. F7 = F7 strike-slip fault, KFZ = Killoran fault zone, MZE = Main zone east normal fault. (C-N) Slices through the block model along the profile, with the major structures indicated as in A and B. Each resource block is 4 × 4 × 12 m.

Downloaded from https://pubs.geoscienceworld.org/segweb/economicgeology/article-pdf/113/7/1455/4558470/1455-1477.pdf
by Univ College Dublin user

of elevated Cu-Ni-Co-Cd-Ag tonnage in both the footwall and hanging-wall orebodies are shown to line up with each other (Kyne et al., 2017). These zones are interpreted to have been one distinct feeder point across the segmented normal faults before reverse reactivation of the fault. Minor amounts of Ni, Ag, Cd, As, and Cu occur locally on other minor ENE-trending normal faults but only in the Waulsortian, notably in Main zone east and north (Fig. 5). Elevated Ni, Cu, or Co is not seen in other parts of the mine.

Total As tonnages correlate well with the distribution of Fe and with the distribution of Cu, Ni, Co, and Ag. This is because As is present in arsenian pyrite and arsenopyrite in the Fe sulfide-rich areas (Hitzman et al., 2002; Wilkinson et al., 2005b) but also as tennantite, niccolite, and arsenopyrite near the feeder zones.

High tonnages of Zn and Pb occur in the hanging wall of the major normal fault segments proximal to these Ni-Cu-As-Ag-Cd-Co–rich points (Figs. 5, 6C, D, I, J). Zn tonnages, however, extend over a much wider area than Pb tonnages. This is reflected in the Zn/Pb and Zn/(Zn + Pb + Fe) ratios, which, in a broad sense, increase north to northeastward away from the normal faults and Ni-Co-Cu-Ag–rich feeders (Figs. 5, 6F, K). Zn/Pb ratios increase from 3:1 proximal to feeder points up to 12:1 distally. Zn/Pb ratios are low (<0.5) close to feeder points and increase both laterally away from the normal fault and vertically away from the base of the Waulsortian.

The Island Pod and Bog zone central orebodies have very high Zn/Pb ratios and significant Zn + Pb contents but lack elevated Cu, Co, and Ag values (Fig. 5). In the Island Pod orebody, east-west normal faults with only minor displacements on the order of several meters occur in both the northern and southern areas of the orebody, separated by a NW-trending monocline (Fig. 5). These structures appear to control the distribution of the ore. In Bog zone central, ore occurs along a hanging-wall breaching fault (the Bog zone central fault) of the relay ramp between Bog zone west and Bog zone east (Fig. 3).

No significant metal tonnages are found updip in the relay ramps between the normal faults (Fig. 3 for relay ramp locations). Moreover, the southeast edges of the Main zone and Derryville orebodies align with the lower edges of the relay ramps (Figs. 3, 5). In the Main zone, an area of particularly elevated Pb tonnages occurs in the orebody at the base of the Main zone-Derryville ramp, coinciding with spots of elevated Ni, Cu, Ag, Co, and Cd tonnages (Fig. 5). Many small normal faults with throws less than 10 m are found in this area and appear to control distribution of ore minerals in this area. Importantly, this zone ("panel 5" in mine terminology) has lesser amounts of pyrite than most other strongly mineralized areas of the mine, which is reflected in low Fe/(Zn + Pb) ratios (Fig. 5). In addition, the panel 5 area shows very low Zn/Cd values and high total Cd content (Fig. 5). Much of the Cd occurs in sphalerite, which generally has a dark-red color (Wilkinson et al., 2005b, 2011). Both Cd and Fe concentrations in sphalerite at Lisheen vary strongly as a function of sphalerite texture, paragenetic timing, and location within the deposit. Sphalerites with elevated Cd concentrations occur paragenetically late or in the Lisduff Oolite orebodies (Wilkinson et al., 2005b). Therefore, areas within the mine with low Zn/Cd and high Cd contents, such as the area at the base of the Main zone-Derryville ramp (Fig. 5), are interpreted to be the product of a late pulse of Cd-rich sphalerite mineralization. Since this area does not fall near any identified feeders on the major normal faults, it is interpreted that fluid pathways changed through time to favor this area in the later stages of orebody formation—perhaps during advanced development and increased displacement on the Main zone-Derryville relay ramp.

Other trends are visible in the metal distributions. The Zn/Pb and Zn/Fe ratios show clear northwest trends that correlate with previously identified NW-trending structures (Fig. 5). In some places areas of elevated Zn/Fe and Zn/Pb coincide, but this is not always the case.

Elevated metal tonnages also occur locally on dextral oblique-slip reverse faults, certainly in the Main zone and Derryville (Figs. 5, 6). As shown in Figure 6, elevated Ni, Cu, Pb, and Zn tonnages in the hanging wall of these oblique-slip reverse faults are interpreted to be the product of dextral offsetting of preexisting zones of elevated metal tonnages near the normal faults. These reverse faults are not significantly mineralized laterally away from the orebodies (Fig. 5).

The orebody is also zoned vertically with Zn/Cu, Zn/Pb, and Fe/Zn increasing from bottom to top (Fig. 6F, L). The vertical Fe/Zn zoning mainly reflects the fact that a pyrite cap is generally found on top of the sphalerite- and galena-rich massive sulfides. Although the highest Zn, Pb, Ni, Cu, Co Cd, Ag, and As values occur generally at or near the base of the Waulsortian, there are some exceptions to this rule. For example, in the Island Pod orebody, the highest values are not at the base of the Waulsortian, occurring some 20 m above its base. In some locations close to the hanging wall of normal faults, two distinct lenses of elevated Zn and Pb occur, above and below areas consisting predominantly of pyrite (e.g., Fig. 6C, D, I, J).

Results—Silvermines Deposit

The Silvermines deposit in County Tipperary has had several centuries of activity, with modern mine life lasting from 1963 until its closure in 1982 for the main Pb-Zn mine and in 1993 for the Ballynoe/Magcobar barite open-cast mine. The main mine area contained 17.7 Mt of ore resource at 6.4 wt % Zn, 2.5 wt % Pb, and 23.0 g/t Ag (Andrew, 1986), of which 11 Mt was mined at 10 wt % Zn + Pb. The Ballynoe/Magcobar barite deposit in the same area produced 5.0 Mt of 85 wt % $BaSO_4$.

Within the main mine area, two stratiform (concordant) orebodies have been identified: G zone upper and B zone (Fig. 7). Ore within these two zones comprises mainly sphalerite, galena, and pyrite replacing carbonates and carbonate breccias near the base of the Waulsortian (Taylor, 1984; Andrew, 1986; Reed and Wallace, 2004). Another stratiform zone of mineralization was identified within the Cooleen zone prospect (Fig. 6; cf. Lee and Wilkinson, 2002). In addition to the concordant orebodies, several zones of Zn-Pb mineralization exist that are discordant to stratigraphy, including G zone lower, K zone (Knockanroe), C zone (Ballygowan South), and P zone (Fig. 7). In these zones, the Zn-Pb mineralization is associated with brecciated carbonates of the Lower Dolomite unit or brecciated sandstones of the Old Red Sandstone (Fig. 7) that are recemented by quartz, sulfides, barite, and carbonates (Rhoden, 1959; Andrew, 1986).

Downloaded from https://pubs.geoscienceworld.org/segweb/economicgeology/article-pdf/113/7/1455/4558470/1455-1477.pdf
by Univ College Dublin user

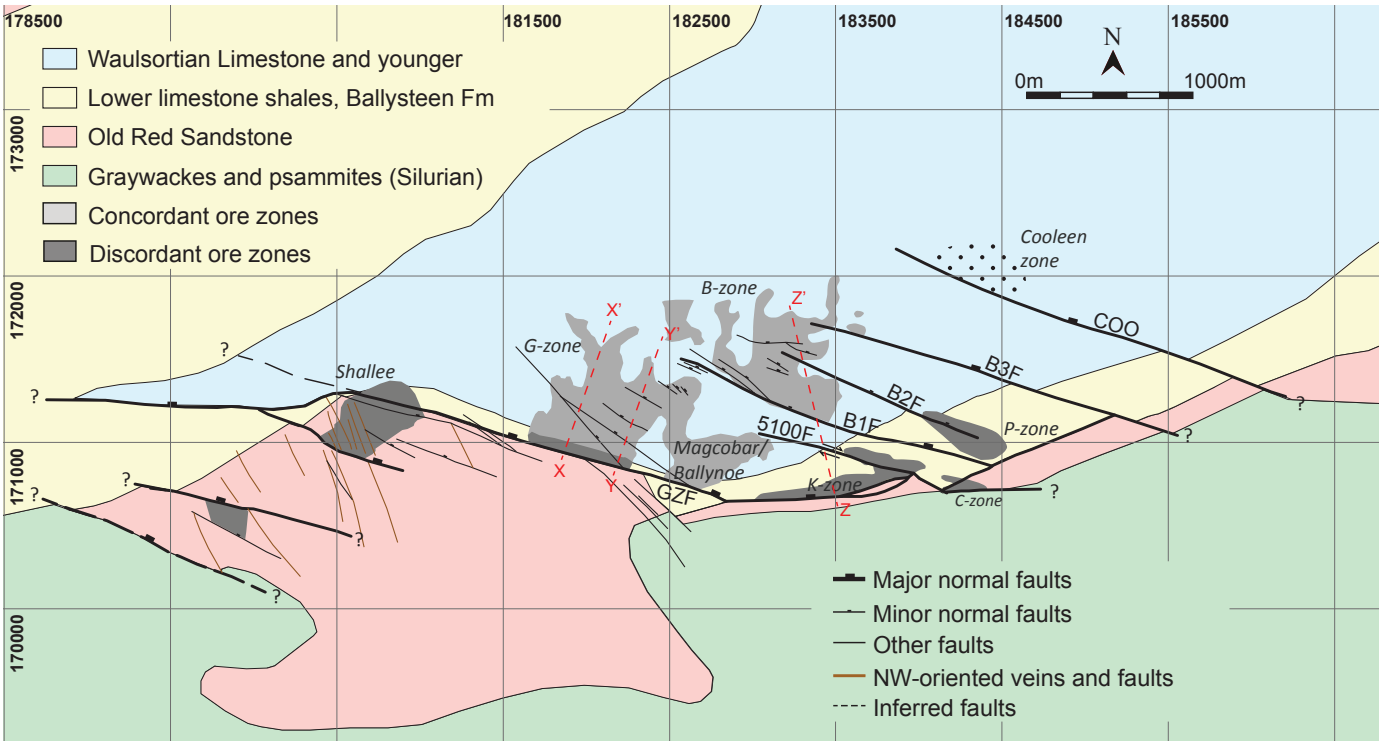

Fig. 7. Simplified surface geologic map of the Silvermines deposit. Grid references are relative to the Irish Grid TM65 datum. Orebodies are mine reserves at 4 wt % Zn + Pb as defined by Andrew (1986) and Irish Base Metals Ltd. Ore zones have been projected to surface and annotated in italics. Faults are in bold and abbreviated as 5100F = 5100 fault, B1F = B zone 1 fault, B2F = B zone 2 fault, B3F = B zone 3 fault, COO = Cooleen fault, GFZ = G zone fault. Section lines X-X', Y-Y', and Z-Z' refer to Figure 10.

Key structural and stratigraphic observations

Figure 7 shows a geologic map of the deposit, highlighting the main structures as interpreted from drilling, mapping, and historical mine data and modeled in 3-D. The structures southwest of Shallee are compiled from other sources (Rhoden, 1959; Taylor, 1984; Andrew, 1986). The Silvermines deposit is located on the southern limb of the open Kilmastulla syncline. The main structures are a WNW-trending array of left-stepping fault segments with maximum displacements between 130 and 375 m, linked by relay ramps (Kyne et al., 2017). These are colloquially referred to as the Silvermines fault zone. The main fault segments from west to east are the G zone fault, B zone faults 1 through 3, and Cooleen fault. Underground structural maps and borehole logs near the G zone and B zone faults show that these are complex fault zones up to 30 m wide, with fault lenses and complex internal bed rotation. Some of the relay ramps are breached, either as a hanging-wall breach (G zone to B zone 1 faults; B zone 1 to B zone 3 faults) or a footwall breach (Shallee). These breaching faults have small displacements (max 40 m) compared to the normal faults (Fig. 7).

Minor WNW-trending normal faults are observed throughout the orebodies with limited lateral extent (<100 m) and throws less than 10 m. These strike parallel to the major normal faults. Regionally, subvertical veins with barite, galena, carbonates, quartz, and tetrahedrite are associated with NW-NNW–trending faults, for example at Shallee, Shallee White, and Gortnadyne/Gorteenadiha (Fig. 7; Rhoden, 1959).

Mineralization and brecciation

A generalized paragenesis for the Silvermines deposit is presented in Figure 8, based on a critical review of several previous studies (Taylor and Andrew, 1978; Andrew, 1986; Mullane and Kinnaird, 1998; Lee and Wilkinson, 2002; Reed and Wallace, 2004, and references therein). Although some conflicting paragenetic interpretations are given by different authors, many of the core observations are similar (Taylor, 1984; Andrew, 1986; Kucha, 1989; Lee and Wilkinson, 2002; Reed and Wallace, 2004). In contrast to Lisheen, the Silvermines deposit experienced less extensive regional dolomitization, hence the host rocks to the Zn-Pb ore are often limestone or limestone breccias. Early diagenetic marine calcite cements are formed prior to any brecciation (Hitzman et al., 1998; Lee and Wilkinson, 2002; Reed and Wallace, 2004). The earliest pyrite at Silvermines shows bacteriogenic $\delta^{34}S$ signatures (Coomer and Robinson, 1976) and is associated with minor sphalerite. The earliest breccia textures recognized at Silvermines rework this pyrite and sphalerite and are referred to by Taylor (1984) and Andrew (1986) as slump breccias or as type I debris-flow limestone breccias by Lee and Wilkinson (2002). Host-rock calcite allochems, early breccias, and calcite cements are sometimes replaced by (Fe)-dolomite and siderite that is concomitant with brecciation, although most of the host-rock and breccia cements are limestone.

These early events were followed by replacement of brecciated carbonates by Fe-Zn-Pb sulfides, producing the bulk of the Zn-Pb ore within the deposit (Kucha, 1989; Lee and

Downloaded from https://pubs.geoscienceworld.org/segweb/economicgeology/article-pdf/113/7/1455/4558470/1455-1477.pdf
by Univ College Dublin user

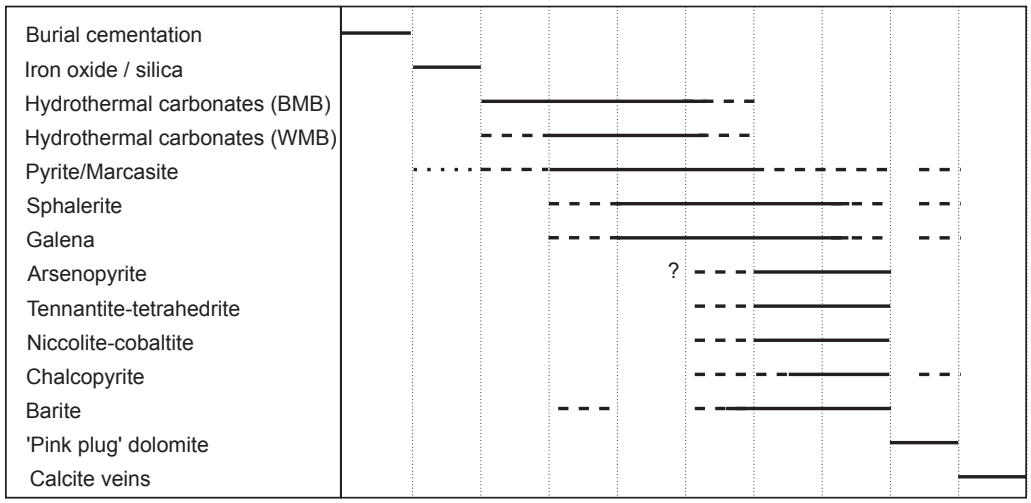

Fig. 8. Generalized paragenesis at Silvermines based on new observations integrated with those of other authors (Taylor and Andrew, 1978; Andrew, 1986; Mullane and Kinnaird, 1998; Lee and Wilkinson, 2002; Reed and Wallace, 2004, and references therein). The BMB and WMB are black matrix breccia and white matrix breccia, respectively, referring to broad categories of types of replacive hydrothermal dolomite in the breccias.

Wilkinson, 2002; Reed and Wallace, 2004). Pyrite, sphalerite, and galena replace breccias in both the concordant and discordant orebodies, occurring predominantly as breccia matrix replacement with corrosion and replacement of clasts where mineralization is pervasive. Multiple brecciation events are recognized (Andrew, 1986; Kucha, 1989; Lee and Wilkinson, 2002). The Zn-Pb orebody is cut by later fracture-hosted sphalerite and galena.

Barite and siderite are also found in significant quantities within the Silvermines deposit, particularly within the Ballynoe/Magcobar barite orebody as well as in certain areas of the B zone. The barite at Ballynoe occurs as microcrystalline acicular crystals and coarse cavity-filling cements, generally very late in the paragenesis (cf. Mullane and Kinnaird, 1998; Reed and Wallace, 2004). Barium is also found in barian feldspar (Andrew, 1986; Kucha, 1989; Lee and Wilkinson, 2002; Reed and Wallace, 2004). Zinc and Pb within the Silvermines deposit occur primarily within sphalerite and galena, respectively. Silver occurs mainly as trace elements in galena, although several Ag sulfosalts have also been identified (Taylor, 1984).

Metal distributions

Figure 9 shows metal distribution maps for Silvermines, including Zn, Pb, and Ag grades as well as Zn/Pb ratios. Three sections perpendicular to the main normal fault segments (south-southwest to north-northeast) are shown in Figure 10: one across the G zone orebody, one through the relay ramp between the G zone and B zone faults and into the B zone orebody, and a final cross section through the K and B zones.

Detailed metal distribution maps in Figure 9 highlight the presence of significant Zn-Pb mineralization at the base of the relay ramps between the G zone and B zone 1 faults and the B zone 1 and B zone 2 faults (Fig. 7). Importantly, while some Zn-Pb mineralization occurs midway up these ramps, most significant metal grades are localized near the base of the ramps. Economic Zn-Pb mineralization is absent in the eastern updip portions of the relay ramps.

At the G zone, low Zn/Pb ratios of 2:1 occur within the fault plane of the normal fault, whereas ratios at the base of the Waulsortian steadily increase north-northeastward away from the fault (Figs. 9, 10A). Limited data at the Cooleen zone show elevated Zn/Pb ratios (>9:1), similar to the most elevated (and distal) values in the G zone orebody. Other authors have previously recognized the increase in Zn/Pb ratio away from the main normal faults as well as an enrichment in Pb along the G zone and B zone faults (Taylor and Andrew, 1978; Taylor, 1984). A longitudinal projection of the G zone orebody near the G fault by Andrew (1986) showed the Zn/Pb ratio increasing from less than one at depth to over four higher up where the discordant orebody intersects the base of the Waulsortian Formation.

Elevated Ag values occur very close to the fault in the Waulsortian and along both major and minor normal faults. The highest Ag values correspond to points with highest Pb values (Fig. 9). Minor chalcopyrite, arsenopyrite tennantite, lollingite, and boulangerite and Pb, Cu, and Ag sulfosalts were found in the fault planes and in the lower dolomite discordant orebody (Andrew, 1986). Taylor (1984) found areas of high concentrations of Cu, As, and Sb sulfosalts, which corresponded to elevated Ag values and low Zn/Pb ratios, within the B zone orebody. No sulfosalts were identified elsewhere in the B zone. For example, the 4500 and 4611 areas of the B zone were seen to contain significant bournonite, boulangerite, jordanite, and a variety of Ag-As minerals (Taylor, 1984). These areas correspond to the hanging-wall area of the fault tips of the B zone 2 and B zone 3 faults intersecting the B zone from the east (Fig. 7).

The Zn/Pb ratios are observed to be elevated in the P zone (>20:1) and moderately elevated in the K zone (12:1) and C zone (10:1), shown in Figure 10C. These orebodies are hosted in the Lower Dolomite unit and are associated with breaching faults or with the intersection of the breaching faults and associated normal faults. Silver values are relatively low in these zones compared to those near the normal faults in the G zone and B zone.

Downloaded from https://pubs.geoscienceworld.org/segweb/economicgeology/article-pdf/113/7/1455/4558470/1455-1477.pdf
by Univ College Dublin user

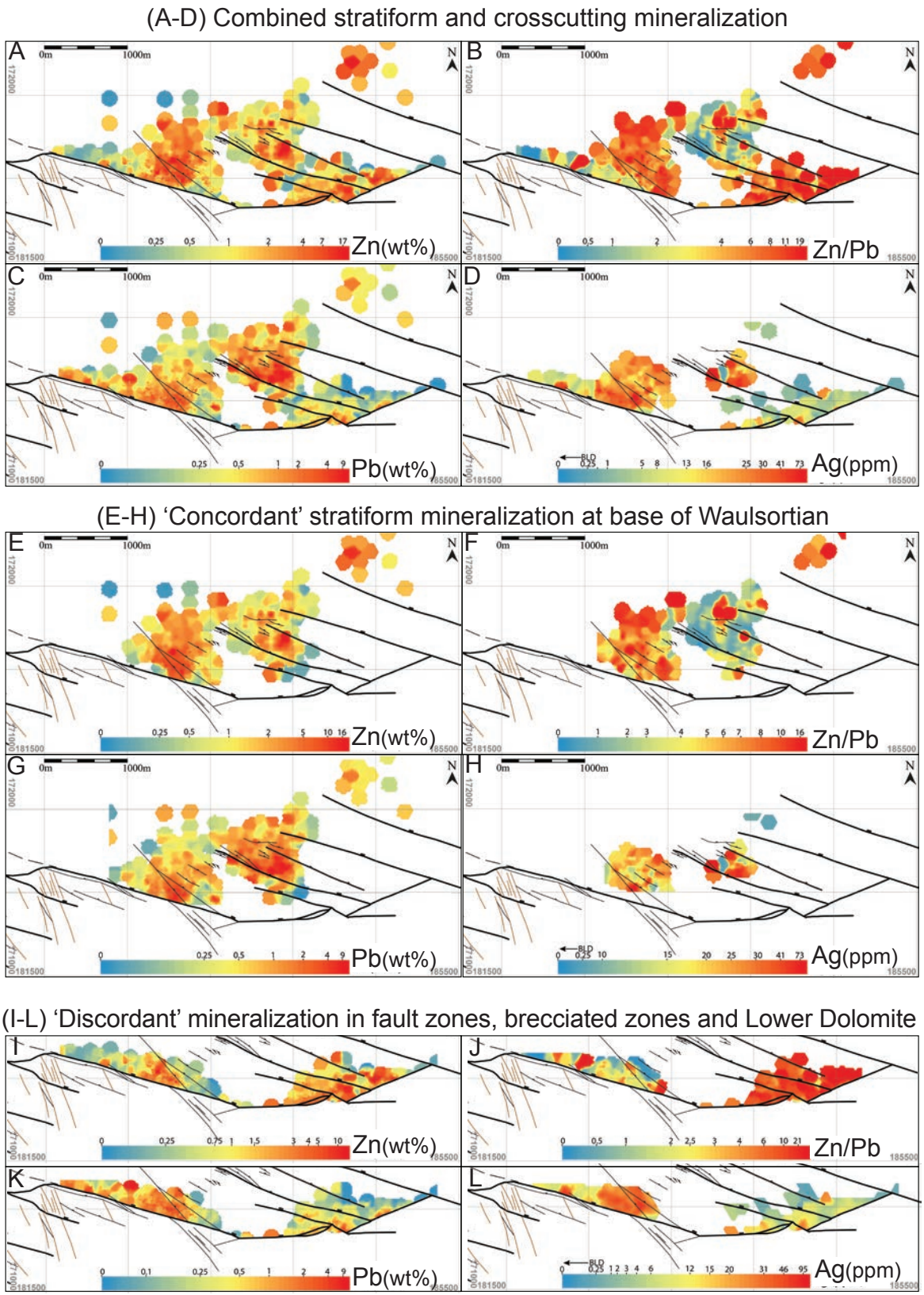

Fig. 9. Metal distribution maps showing Pb, Zn, and Ag concentrations and the Zn/Pb ratio at Silvermines. Two types of orebodies are present at the deposit: stratiform orebodies at the base of the Waulsortian (concordant ore) and discordant orebodies in fault zones, brecciated zones, and the Lower Dolomite unit. (A-D) show metal distribution maps of the full assay data set, (E-H) only show assays of concordant ore, and (I-L) only show assays from discordant orebodies. All elemental distributions of Zn and Pb are in weight percent and of Ag in pm; see methodology section for details on generation of these maps.

Downloaded from https://pubs.geoscienceworld.org/segweb/economicgeology/article-pdf/113/7/1455/4558470/1455-1477.pdf
by Univ College Dublin user

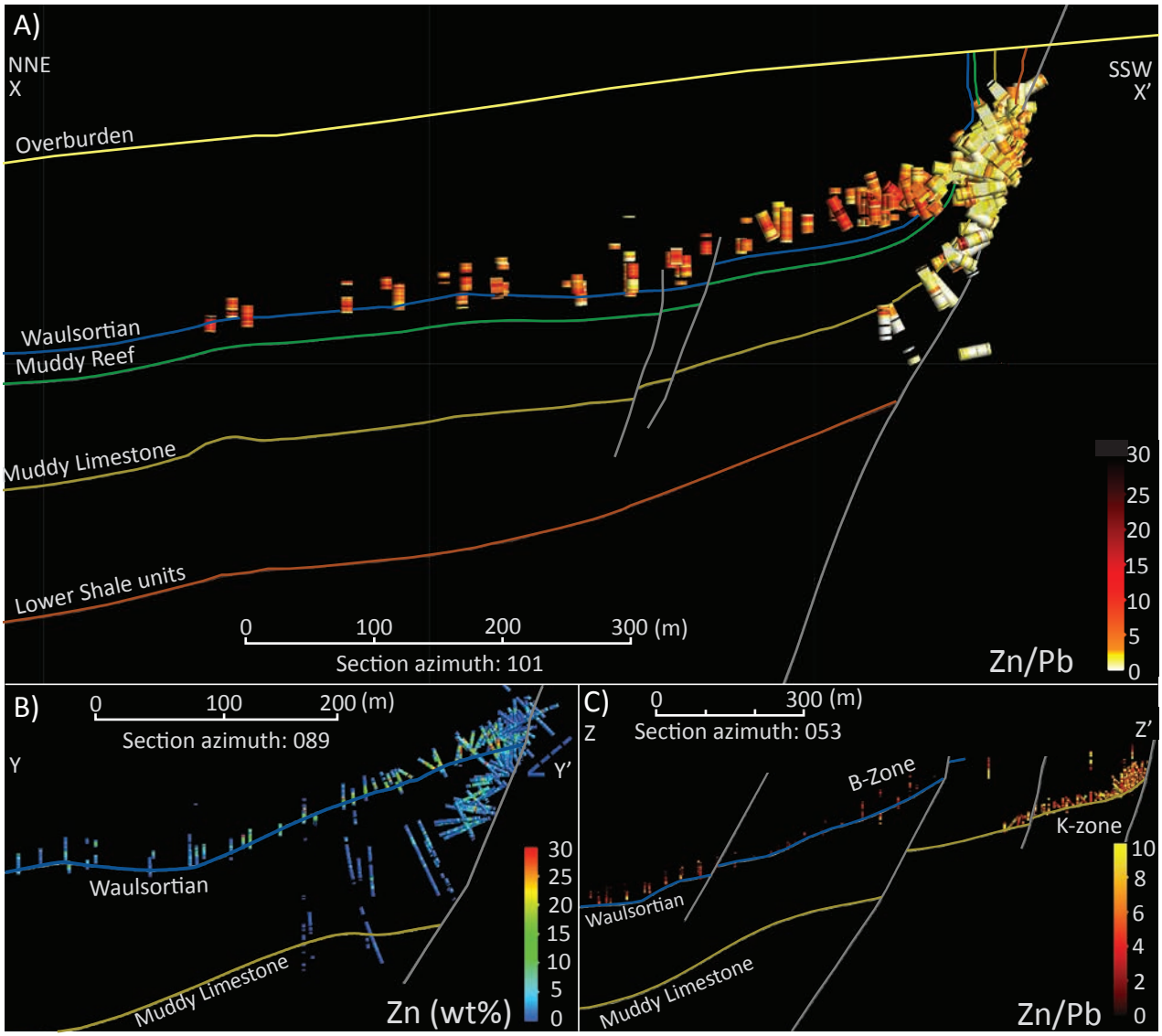

Fig. 10. Cross sections through the orebodies at Silvermines (see Fig. 7 for location). Faults are indicated in gray. (A) Cross section X-X' shows Zn/Pb ratio with low values (in white to yellow colors) along the Silvermines fault plane (discordant ore) and an increasingly higher Zn/Pb ratio (in orange-red colors) away from the fault in the ore at the base of the Waulsortian (concordant ore). (B) Cross section Y-Y' shows Zn distribution in the concordant and discordant orebody at G zone. The highest Zn grades (in green colors) are located at the base of the Waulsortian near the G zone fault. (C) Cross section Z-Z' shows elevated Zn/Pb values (in orange to yellow colors) in K zone, where the ramp-breaching fault intersects the 5100 and B zone faults. Mineralization in this area is located at the base of the Lower Dolomite unit. Much lower Zn/Pb values are seen in B zone, where the ore is hosted at the base of the Waulsortian.

Discussion

Distinct points along segmented normal fault arrays are identified as feeders to many of the orebodies within both the Lisheen and Silvermines deposits. Here, fluids spill out into the hanging wall near the base of the Waulsortian. These feeders control the location of the orebodies along various fault segments. Generally, these feeder zones are characterized by elevated Zn and Pb tonnages (decreasing outward), low Zn/Pb ratios (increasing outward), and elevated Ni, Ag, Cu, Co, and As (decreasing rapidly outward). Mineral assemblages of tennantite, niccolite, cobaltite, chalcopyrite, and Ag sulfosalts are found in close proximity to these points along the normal faults. These minerals generally only occur in accessory quantities elsewhere within the mineralized zones. Vertical zonations are also observed within the orebody, with Zn/Cu, Zn/Ba, Zn/Pb, Fe/Zn, and Zn/(Zn + Pb) increasing upward, mimicking the horizontal variation (Fig. 6F, L).

The metal zonations emanating from feeders can be well explained in terms of changes in temperature, pH, and oxygen fugacity (Anderson, 1975; Barnes, 1983; Sverjensky, 1986; Anderson and Garven, 1987; Cooke et al., 2000). Given the clear existence of feeder zones, proximal-distal signals are interpreted to arise primarily from mixing of hot, medium-salinity metalliferous fluids and low-temperature, high-salinity brines, resulting in reduced metal solubility and

Downloaded from https://pubs.geoscienceworld.org/segweb/economicgeology/article-pdf/113/7/1455/4558470/1455-1477.pdf
by Univ College Dublin user

precipitation from the point of initial mixing outward (Banks et al., 2002; Corbella et al., 2004; Wilkinson et al., 2005a, b; Anderson and Thom, 2008; Wilkinson, 2010). For Lisheen, this is corroborated by the net enrichment/depletion patterns of several (trace) elements that trend away from the normal faults. These patterns are interpreted as the result of progressive dissolution-precipitation processes during fluid mixing (Wilkinson et al., 2011).

Several pyrite generations are observed predating, contemporaneous with, and postdating sphalerite and galena mineralization at Lisheen (Redmond, 1997; Fusciardi et al., 2004; Wilkinson et al., 2005b) as well as at Silvermines (Andrew, 1986; Lee and Wilkinson, 2002). Although these timing differences do slightly complicate the interpretation of Fe metal distributions with respect to identifying feeders, most of the pyrite has been identified as being precipitated before the main Zn + Pb ore in the paragenesis. The paragenetically early pyrites at Lisheen have $\delta^{34}S$ signatures (–38.1 to –44‰) with very high fractionations relative to their presumed seawater sulfate source of $\delta^{34}S$ = 14 to 22‰ (Claypool et al., 1980), which is indicative of bacteriogenic sulfate reduction at low depths (Hitzman et al., 2002; Wilkinson et al., 2005b). At Lisheen the massive pyrite caps overlying Zn + Pb-rich lenses are strongly controlled by the early east-northeast faults, and this is reflected in the Fe distribution maps, which show a strong affinity with the hanging walls of both major and minor normal faults (Fig. 5). This distribution clearly indicates the strong control of early EW-trending (Lisheen) or WNW-trending (Silvermines) faults on early pyrite precipitation, potentially providing an accessible sulfur source for later sulfide mineralization.

Certain minerals, such as niccolite, cobaltite, tennantite-tetrahedrite, chalcopyrite, and barite, are seen to precipitate late in the paragenesis relative to pyrite, sphalerite, and galena near the feeders (Figs. 4, 8). The progressive waxing and waning of temperature and salinity of the hydrothermal fluid entering through the feeder zones can explain the paragenetically later position of chalcopyrite, niccolite, and other minerals that require higher temperatures or increased salinities to be soluble (e.g., Yardley, 2005). The most likely case is that certain metals were only introduced into the system when their solubilities in the hydrothermal fluid were high enough.

Previous studies have suggested that feeders and orebodies in Irish-type deposits are located at points of maximum throw along normal faults (Johnston et al., 1996; Shearley et al., 1996; Hitzman, 1999; Hitzman et al., 2002). The 3-D modeling and distribution maps in this study clearly show that the feeders occur at points of high displacement on the normal faults but not necessarily at areas of maximum displacement. In simple terms, the feeders occur where there is sufficient displacement either to cause juxtaposition of favorable units and/or to generate fault rock and increased complexities (cf. Childs et al., 1995; Walsh et al., 1999, 2003; Bonson et al., 2012).

In the case of intact or breached ramps with low displacement, feeders are located at the base of the relay ramps (Main zone east-Derryville and Derryville-Bog zone west ramps at Lisheen in Fig. 3 and G zone-B zone 1 and B zone 1-B zone 3 fault ramps at Silvermines in Fig. 7). Here, ramp geometries strongly affect orebody geometries, with stratiform orebodies at both deposits extending along, and parallel to, the base of relay ramps but not updip on the ramps (Fig. 11A). This suggests a form of bathymetric control on localization of mineralization. In terms of fluid flow and sulfur sources for precipitation, this could indicate that the dense brines and/or preexisting pyrite bodies were located in the bathymetrically depressed hanging walls of normal faults at the base of relay ramps. Conversely, where relay ramps are strongly breached and intensely fractured, such as the relay ramp between Main zones east and west at Lisheen (Fig. 3), feeders occur in the relay ramps themselves where fluids are interpreted to have been focused upward through the fractured relay ramps (Fig. 11C). The brittle faulting/fracturing that results from accommodation of the bending and extension of the ramps is often seen to locally alter porosity and permeability and increase structural complexity (Ferrill and Morris, 2001; Rotevatn et al., 2007; Rotevatn and Bastesen, 2012; Fachri et al., 2013), giving rise to structurally enhanced permeability (Cox et al., 2001; Cox, 2005; Faulkner et al., 2010). In the case of breaching faults bounding largely intact relay ramps, such as in the Bog zone west and central at Lisheen, fluids are focused toward and into the breaching faults (Fig. 11B). Breached relay zones have been identified as potentially excellent vertical fluid conduits in tight carbonate rocks (Bonson et al., 2007; Bastesen and Rotevatn, 2012; Rotevatn and Bastesen, 2012). Hence, although the feeders are always located at locations of high displacements along the faults, the exact location of the feeder zones is strongly dependent on local factors, the scale of the fault system, and how the fault network has developed through time.

In addition to the structural setting, the interplay of the stratigraphic and normal fault architecture is interpreted to strongly influence fluid pathways for upwelling metal-bearing hydrothermal fluids (see Fig. 11 for a visual explanation). The Carboniferous normal faults have been interpreted to continue down into the basement rocks, often reactivating or being localized along preexisting structures (e.g., Johnston et al., 1996; Johnston, 1999; Worthington and Walsh, 2011; Bonson et al., 2012). At Lisheen minor mineralization occurs in the Lisduff Oolite Member wherever it was juxtaposed with the Waulsortian at the time of mineralization (Shearley et al., 1996; Redmond, 1997; Hitzman et al., 2002; Fusciardi et al., 2004; Kyne et al., 2017). The orebodies in the Lisduff Oolite Member are spatially very restrictive and characterized by locally elevated Zn + Pb tonnages, low Zn/Pb ratios, and elevated Cu, Ni, Co, Ag, and As values, similar to the metal zonations present in the feeder zones themselves. At the feeder point where the two brittle juxtaposed units touch, the cool saline brines are brought into contact with the hot, buoyant, metalliferous hydrothermal fluid, inducing mixing and precipitation (Fig. 11).

Other structural trends, besides those exerting control over feeder points, control metal distribution within individual orebodies (Fig. 12). At Lisheen, a clear link is seen between northwest trends in Zn/Pb and Zn/Fe ratios and early pre-Variscan NW-trending low-displacement structures. A particularly good example of this can be seen in the Main zone and Derryville orebodies at Lisheen (Fig. 5). These northwest trends are very similar to those observed at Galmoy located to the northeast of Lisheen (Lowther et al., 2003). At Lisheen, these northwest structures correspond to areas of different

Downloaded from https://pubs.geoscienceworld.org/segweb/economicgeology/article-pdf/113/7/1455/4558470/1455-1477.pdf
by Univ College Dublin user

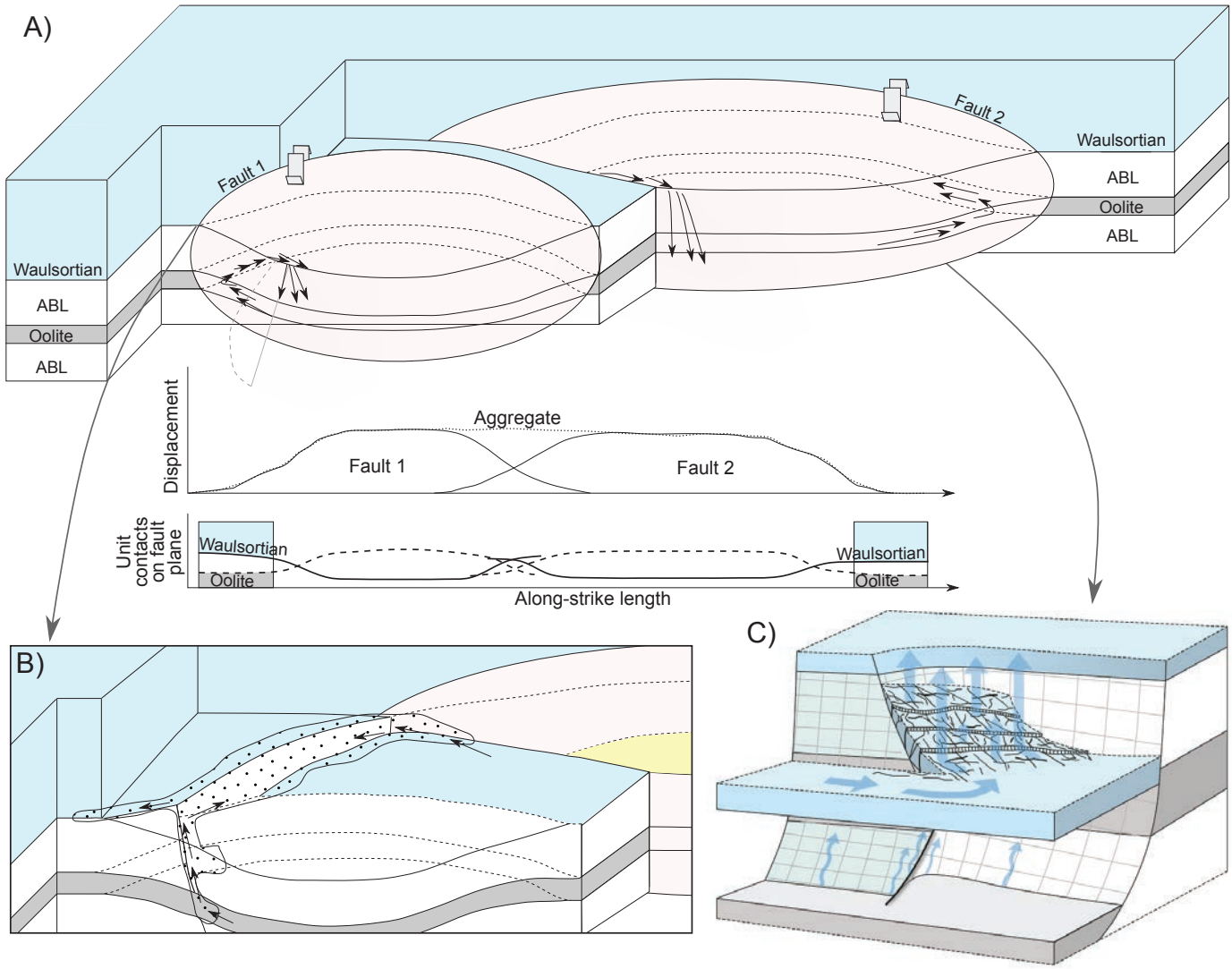

Fig. 11. Interpretative schematic for fluid flow in segmented fault arrays forming orebodies at Lisheen and Silvermines. (A) Certain brittle and permeable units can act as natural fluid focusers and serve as (lateral) conduits for along-fault fluid flow (see arrows). Depicted here is the Oolite Member at Lisheen, but the same concept applies for fault rock breccias, certain units in the Old Red Sandstone, or the Lower Dolomite unit at Silvermines. Feeders to the orebodies then occur where the sulfur-poor metal-bearing hydrothermal fluids mix with a cooler, saline, sulfur-rich brine or a stock of reduced sulfur (e.g., pyrite) at the base of the Waulsortian. The fault architecture can serve to bring fluid-focusing units into contact with the Waulsortian. In intact ramps at Lisheen, this occurs systematically where the Waulsortian is brought into juxtaposition with the Oolite Member. (B) Blow up schematic of the fault breccias and brecciated carbonate units along breaching faults and up-ramp parts of the fault zones serving as distal traps for the fluids, closely confined to the fault zones. (C) Smaller-scale, strongly breached relay ramps are highly fractured zones and conduits for up-fault fluid flow (modified after Kyne et al., 2017). They also serve as traps for mineralization. ABL = argillaceous bioclastic limestone.

Zn/Pb values relative to background values away from the main structures. This is interpreted to be the result of these northwest structures serving as preferable fluid conduits, allowing the fluid mixing front to extend farther into the hanging wall from the feeder site than typically would be expected (illustrated in Fig. 12). The same mechanism would serve to extend the fluid mixing front along minor EW-NE–trending normal faults at Lisheen or NE-trending faults at Silvermines.

Variscan reactivation of normal faults and the formation of transpressional faults and folds complicate the original normal fault architecture (Coller, 1984; Johnston et al., 1996; Hitzman, 1999; Kyne et al., 2017). These fault zones are mineralized where they crosscut Zn-Pb orebodies. A good example occurs within the Bog zone at Lisheen where the Bog zone east transpressional fault duplicates the Bog zone east orebody, cutting the orebody into two and moving the western portion dextrally over the top of the eastern portion (Kyne et al., 2017). Mineralization within the Bog zone transpressional fault only occurs where it is in direct contact with the Bog zone east orebody. Metal distributions are displaced by these faults in the direction of movement, the extent of which is proportional to the amount of movement on the faults. The clearest example of this occurs within the dextral oblique Derryville transpressive fault, where anomalously

Downloaded from https://pubs.geoscienceworld.org/segweb/economicgeology/article-pdf/113/7/1455/4558470/1455-1477.pdf
by Univ College Dublin user

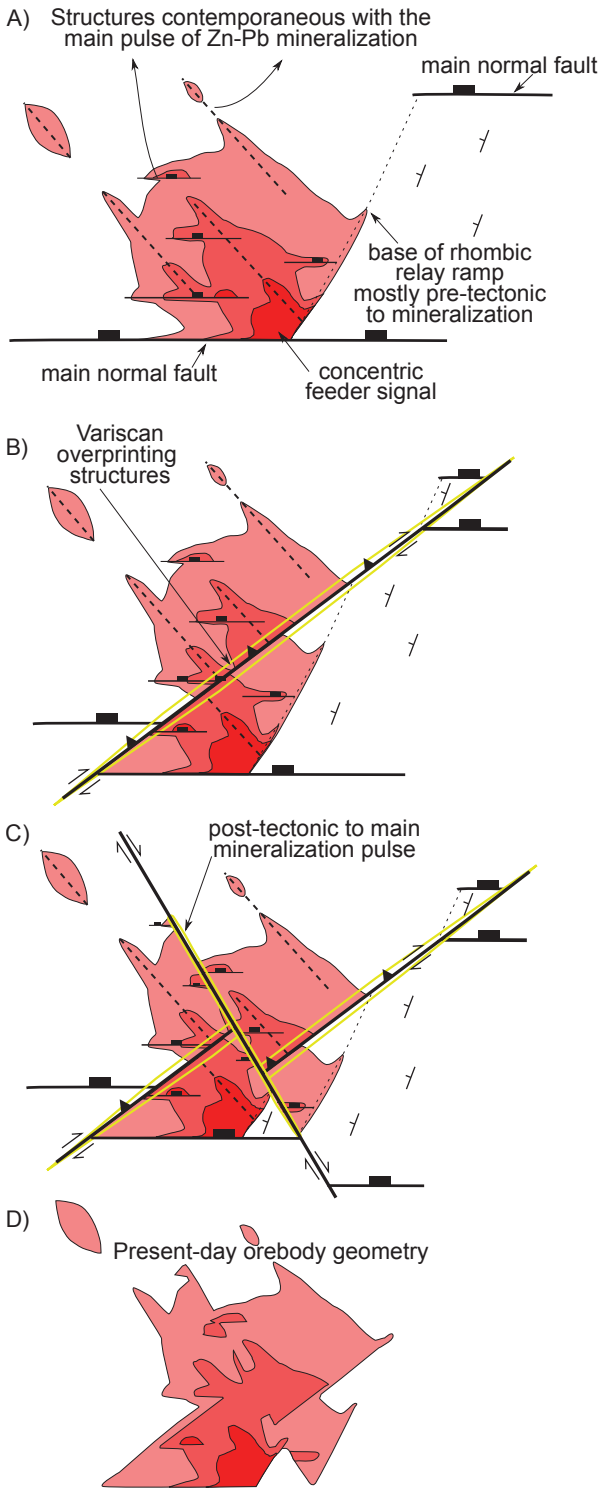

Fig. 12. Generic schematic drawing representing the evolution of structural controls on present-day orebody geometries, location of feeders, and metal distribution trends at Lisheen and Silvermines. (A) Situation during extensional tectonics, including the development of northwest structures. (B) Variscan reverse fault structures, reactivation of normal faults, and folding. Note the zone of influence of the transpressional faults on displacing and concentrating mineralization, highlighted in yellow. (C) Post-Variscan strike-slip faulting. (D) Schematic representation of present-day orebodies after structural modifications. Orebodies and metal distributions can be heavily influenced by several structural modifications and, in the case of Lisheen, must be reconstructed to show the true nature of metal distributions.

high concentrations of Fe, Zn, Pb, Cu, Ni, and As occur in the hanging wall of the fault (Figs. 5, 6A). These concentrations are a result of the movement of the Derryville transpressive fault (~160-m strike-slip component) as determined from the offsets of the normal faults (Fig. 3). To the southwest on the same fault, no significant metal contents are observed (Fig. 5). The Variscan structures therefore mainly serve to simply displace or smear preexisting orebodies.

Importantly, significant orebodies without typical feeder signal are found in both of the deposits (Fig. 12). The Island Pod at Lisheen is characterized by high Zn, very high Zn/Pb values, and low Ni, Cu, Ag, and As values. Bog zone east shows high Ni values but does not exhibit elevated Cu and high Zn/Pb values. In the case of the Island Pod, a NW-trending flexure or monocline and two normal faults appear to be the primary controls (Fig. 3). At Silvermines, there are a number of examples where mineralization is not associated with feeders but located along and close to fault planes in highly fractured zones of breaching faults—certainly close to intersections with the normal faults (Fig. 7). This includes K zone, P zone, and C zone, which are characterized by very high Zn/Pb ratios and low Ag contents compared to the feeder signals in G zone and B zone (Fig. 9). These areas are often structurally complex and interpreted to be distal orebodies, representing either the farthest extent reached by the ore-forming fluids or forms of remobilization of preexisting ore from more proximal locations.

The data sets available for Lisheen and Silvermines are quite different, with a multielement database on the one hand and digitized legacy assay data of only a few elements (Pb, Zn, Ag) on the other. The 3-D structural and horizon modeling of the Silvermines legacy data shows that fundamental insights into the structural framework and its influence on fluid flow pathways can be gained from such data sets. A drawback of the Silvermines data is the absence of density measurements, preventing the creation of detailed block models, which have proven very useful in analyzing fluid flow pathways at Lisheen.

Comparison with other deposits

There are a number of other sediment-hosted deposits, both within the Irish ore field and in other areas, that show metal and structural trends similar to those found within both Lisheen and Silvermines.

Galmoy: At the Galmoy deposit, located ~9 km northeast from the Lisheen orebody, zones of high Zn/Pb are oriented northwest in the CW and K orebodies (Lowther et al., 2003). In both orebodies these trends are associated with NW-oriented structures. Lower Zn/Pb values and significant pyrite are seen in the G orebody in the hanging wall of a major N-dipping normal fault. This potentially indicates that the northwest trends are a distal expression of the feeder zone located on this normal fault bounding the G orebody to the south, a scenario similar to the metal distributions at Lisheen and Silvermines.

Navan: Another important mine within the Irish ore field is the world-class 120 Mt Navan Zn-Pb deposit (Fig. 13), whose metal distributions have been studied by several workers (Andrew and Ashton, 1985; Blakeman et al., 2002; Davidheiser-Kroll, 2014; Ashton et al., 2015). The ore is hosted mainly in the Meath Formation (Pale Beds) of the Navan

Downloaded from https://pubs.geoscienceworld.org/segweb/economicgeology/article-pdf/113/7/1455/4558470/1455-1477.pdf
by Univ College Dublin user

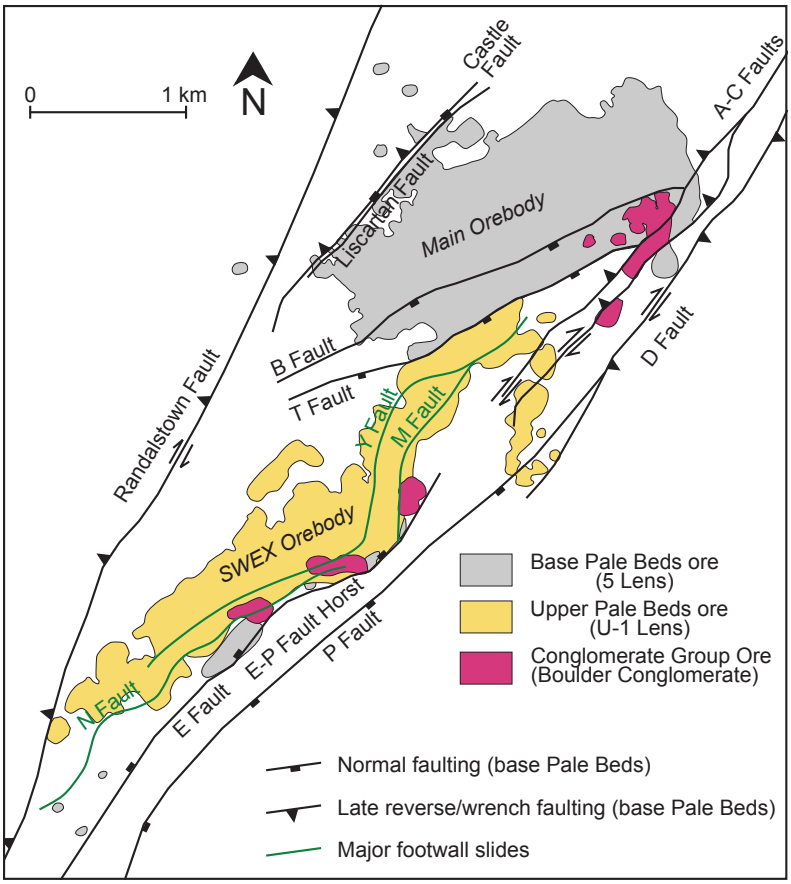

Fig. 13. Structural plan showing the distribution of the principal ore lenses and faults at Navan, as mentioned in the text. Modified from Ashton et al. (2015). For references to stratigraphy refer to Figure 2.

Group, a varied sequence of micritic, oolitic, and bioclastic grainstones, calcareous sandstones, and siltstones (Fig. 2). The structural setting of the Navan deposit is complex (Fig. 13): early ENE-trending normal fault segments (E, P, T, B, Castle faults) in the footwall of a major tilted block, bounded to the south by the Navan fault, are later complicated by SE-extensional low-angle slides and SE-dipping faulting (M, N, Y faults) due to gravitational instability during footwall uplift. The gravitational sliding has led to the creation of a local erosional surface with the Boulder conglomerate unit at its base. All faults are complicated further by later reverse, wrench, and strike-slip tectonics (A-D faults, Randalstown and Liscartan faults).

In the main orebody, elevated Zn + Pb trends lie parallel to, and in the hanging wall of, NE-trending normal faults or fracture zones (recognized early on by Andrew and Ashton, 1985; Blakeman et al., 2002); Zn/Pb ratios decrease westward, and Fe concentrations are highest to the northeast. Clear Fe-rich areas (mainly pyrite) are seen in the hanging wall of early normal faults. In the SWEX ore zone to the southwest of the main ore zone (Fig. 13), high Zn and Pb areas parallel NE-trending normal faults and slide complexes. The early extensional normal E fault was interpreted as the principal controlling structure (Ashton et al., 2015). No strong trends in Zn/Pb ratios are seen, with values lying quite monotonously around four within the E fault. Several elevated hot spots of Zn + Pb + Fe are found along the E fault in areas where the Pale Beds are directly below and in contact with the Boulder conglomerate. Here, the Boulder conglomerate is locally mineralized with high concentrations of pyrite (the Conglomerate Group ore; Fig. 13). Davidheiser-Kroll (2014) attributed the metal distributions here as areas of upward and lateral fluid flow both along NE-trending normal faults and through areas where the Pale Beds are directly below and in contact with the Boulder conglomerate. In that sense, the juxtaposition between these two units is like that between the Waulsortian and Lisduff Oolite at Lisheen.

In contrast to Lisheen and Silvermines, the areas with the highest Zn + Pb content at Navan do not systematically correspond to low Zn/Pb values. At Navan, however, other processes could have added to the complexity of metal distributions, such as the association of metal tonnage hotspots juxtaposed with ore hosted in the Boulder conglomerate and the different lithology of the Navan Group compared to Waulsortian-hosted deposits. In addition, the Navan deposit as a whole lies in a complexly faulted footwall block to the major Navan fault, whereas Lisheen and Silvermines are located in the hanging wall of major fault structures. Nonetheless, elevated Zn, Pb, and Fe values at Navan are strongly associated with the hanging walls of NE-trending normal faults, showing clear zonation from several points along the faults (cf. detailed metal distribution maps of Davidheiser-Kroll, 2014; Ashton et al., 2015). This means that, similar to the Waulsortian-hosted deposits, like Lisheen and Silvermines, normal faults and the bathymetry they create are key in controlling metal distributions at Navan.

Vent-proximal SEDEX deposits: Vent-proximal sedimentary exhalative (SEDEX) deposits are characterized by increasing

Downloaded from https://pubs.geoscienceworld.org/segweb/economicgeology/article-pdf/113/7/1455/4558470/1455-1477.pdf
by Univ College Dublin user

Zn/Pb values and decreasing Zn/Fe, Zn/Ba, and Pb/Fe values away from vent zones or fault breccias (e.g., Goodfellow et al., 1993; Large et al., 2005; Goodfellow and Lydon, 2007; Wilkinson, 2014). Typical sulfide zonations are seen successively precipitating, in order of proximity, chalcopyrite, pyrrhotite galena to sphalerite, and pyrite, most distally within the deposit. Chalcopyrite, galena, and sphalerite zonations mainly reflect a thermal gradient with respect to solubilities. In particular, Sb, Bi, As, and Hg in sulfosalts and arsenopyrites and Ag in sulfosalts and galena occur near the vent complexes.

The similarities in metal zonations between feeders in Irish Zn-Pb deposits and vent-proximal SEDEX deposits around the world can be explained by the fact that in both cases metal zonations originate from mixing of two end-member fluids, similar to those in Irish-type deposits, near a point source along faults. It has been noted that geochemical and metal zoning in other Mississippi Valley-type deposits is generally not strongly developed (Leach et al., 2010). Our study clearly shows that internal zonations can be developed in Irish-type ore deposits.

Conclusions and Implications for Exploration and Mining

Distinct points along segmented normal fault arrays are interpreted to be feeder zones to the Silvermines and Lisheen orebodies. At these points, metal-bearing hydrothermal fluids entered the hanging-wall host rock, generally near the base of the Waulsortian. These feeder points are usually characterized by elevated Zn and Pb tonnages (decreasing outward), low Zn/Pb ratios (increasing outward), and elevated Ni, Ag, Cu, and As concentrations (decreasing rapidly outward). High total metal tonnages exist proximally to the feeders, including mineral assemblages of tennantite, niccolite, chalcopyrite, and sulfosalts, which only occur in accessory quantities elsewhere within the mineralized zones. Vertical zonations are also observed within the orebody, with Zn/Cu, Zn/Ba, Zn/Pb, Zn/(Zn + Pb), and Fe/(Zn + Pb) ratios increasing upward. The metal zonations emanating from feeders in Irish Zn-Pb deposits can be explained by mixing of a buoyant, hot, saline, metalliferous hydrothermal fluid with a colder, dense, sulfur-rich brine in bathymetric lows. The feeders, found at locations of high but not necessarily maximum displacement along the faults, are strongly dependent on the scale and the way the local fault network has developed through time.

Minor mineralization occurs in certain units that are in juxtaposition with the Waulsortian across faults at the time of mineralization. The orebodies in these other carbonate units are spatially very restrictive and characterized by locally elevated Zn + Pb tonnages, low Zn/Pb ratios, and elevated Cu, Ni, and As values—similar to the feeders. Brittle and permeable units can provide fluid pathways for hot buoyant hydrothermal fluids to migrate and focus into, both vertically and laterally. In addition, certain highly fractured and breached relay ramp zones serve as zones of up-fault fluid flow. Feeders to the orebodies occur where the hot, sulfur-poor, metal-bearing hydrothermal fluids mix with a cooler, saline, sulfur-rich brine or interact with a stock of reduced sulfur (e.g., pyrite) at base of the Waulsortian.

Identifying and understanding segmented normal fault arrays and the interplay with stratigraphy is paramount when locating the often-tiny bullseyes that characterize high-tonnage orebodies of the Irish-type Zn-Pb deposits. In general, most of the high-grade/tonnage orebodies in Lisheen and Silvermines are not found within intact relay ramp zones themselves but are localized along their corresponding normal fault segments at those parts of the deposit that were locally bathymetrically deep because of normal faulting. To a certain degree, metal ratio data, such as Zn/Pb and Zn/Ba, and trace element concentrations, such as Ni, Co, As, and Cu, can be useful in vectoring toward the bounding faults as well as in delineating feeder zones characterized by high tonnages and high grades.

Besides the controls exerted by normal faults and feeders on metal zonation, many other structural trends control metal distribution at the scale of the individual orebodies. This study shows that metal distributions are complicated either during mineralization due to differences in metal and ligand solubility or the complex structural evolution of mineral deposits, and/or after mineralization by later structures, which displace existing metal zonations. Careful assessment of whether structures in drill core are cogenetic with or postdate mineralization is thus paramount in successfully interpreting metal distributions regionally.

Importantly, other areas with elevated Zn + Pb but without the typical feeder signal are found in both deposits (such as the Island Pod at Lisheen and K zone at Silvermines). These orebodies are characterized by very high Zn/Pb, Zn/(Zn + Pb), and Zn/Fe ratios. Importantly, they are structurally controlled and occur at the intersection of breaching faults with normal faults or along northwest structural trends. These are interpreted to represent distal but significant orebodies, possibly representing the farthest extent reached by the ore-forming fluids or remobilization of ore from more proximal locations.

This paper therefore highlights the fundamental structural controls that segmented normal fault arrays have on the localization of mineralization and metal distributions within Irish-type Zn-Pb deposits. It also highlights the complex nature of fluid flow pathways through time. Despite significant complexities, analyzing the metal distributions in relation to the structural framework can give many important insights into the controls on and fluid pathways within Zn-Pb orebodies.

Acknowledgments

The authors would like to thank Steve Hollis, Aileen Doran, Julian Menuge, John Conneally, Oakley Turner, Sean Johnson, Annraoi Milner, Michael Philcox, John Murray, Colin Andrew, Bruce Gemmell, David Broughton, Sarah Gleeson, John Ashton, and Claire Chamberlain for insights and fruitful discussion on the structural and stratigraphic framework, metal distributions, and geochemical conditions at the deposits. We are grateful to Chris Bonson and Colin Andrew for providing materials on Silvermines and thank Vedanta Resources for the use of data and drill core from the Lisheen mine. The Geological Survey Ireland and the Exploration and Mining Division are acknowledged for providing regional data and background information for our 3-D modeling efforts, including access to Silvermines drill core. We also thank ARANZ Geo, Paradigm, Mira Geoscience, Midland Valley Exploration, Maptek, and ESRI for providing support and academic licenses of software

Downloaded from https://pubs.geoscienceworld.org/segweb/economicgeology/article-pdf/113/7/1455/4558470/1455-1477.pdf
by Univ College Dublin user

essential to this project. This publication has emanated from research supported in part by a research grant from Science Foundation Ireland (SFI) under grant number 13/RC/2092 and is cofunded under the European Regional Development Fund and by iCRAG industry partners. We thank all iCRAG industry partners for their feedback, support, and provision of associated data sets. Part of the work was carried out as part of Marie Skłodowska-Curie grant agreement no. 745945, funded from the European Union's Horizon 2020 research and innovation program. Finally, the authors would like to thank Ross Large and Patrick Redmond for their helpful and constructive reviews and Larry Meinert for editorial handling.

REFERENCES

Allan, U.S., 1989, Model for hydrocarbon migration and entrapment within faulted structures: American Association of Petroleum Geologists (AAPG) Bulletin, v. 73, p. 803–811.

Anderson, G.M., 1975, Precipitation of Mississippi Valley-type ores: Economic Geology, v. 70, p. 937–942, doi: 10.2113/gsecongeo.70.5.937.

Anderson, G.M., and Garven, G., 1987, Sulfate-sulfide-carbonate associations in Mississippi Valley-type lead-zinc deposits: Economic Geology, v. 82, p. 482–488, doi: 10.2113/gsecongeo.82.2.482.

Anderson, G.M., and Thom, J., 2008, The role of thermochemical sulfate reduction in the origin of Mississippi Valley-type deposits. II. Carbonate-sulfide relationships: Geofluids, v. 8, p. 27–34, doi: 10.1111/j.1468-8123.2007.00202.x.

Andrew, C., and Ashton, J., 1985, Regional setting, geology, and metal distribution patterns of Navan orebody, Ireland: Institution of Mining and Metallurgy Transactions, Section B: Applied Earth Science, v. 94, p. 66–93.

Andrew, C.J., 1986, The tectono-stratigraphic controls to mineralization in the Silvermines area, County Tipperary, Ireland, *in* Andrew, C.J., Crowe, R.W.A., Finlay, S., Pennel, W.M., and Pyne, J.F., eds., Geology and genesis of mineral deposits in Ireland: Dublin, Irish Association for Economic Geology, p. 377–417.

Ashton, J.H., Blakeman, R.J., Geraghty, J.F., Beach, A., Coller, D., Philcox, M.E., Boyce, A.J., and Wilkinson, J.J., 2015, The giant Navan carbonate-hosted Zn-Pb deposit: A review, *in* Archibald, S.M., and Piercey, S.J., eds., Current perspectives on zinc deposits: Dublin, Irish Association for Economic Geology, p. 85–122.

Banks, D.A., and Russell, M.J., 1992, Fluid mixing during ore deposition at the Tynagh base-metal deposit, Ireland: European Journal of Mineralogy, v. 4, p. 921–931.

Banks, D.A., Boyce, A.J., and Samson, I.M., 2002, Constraints on the origins of fluids forming Irish Zn-Pb-Ba deposits: Evidence from the composition of fluid inclusions: Economic Geology, v. 97, p. 471–480, doi: 10.2113/gsecongeo.97.3.471.

Barnes, H.L., 1979, Solubilities of ore minerals, *in* Barnes, H.L., ed., Geochemistry of hydrothermal ore deposits: New York, Wiley, p. 404–454.

——1983, Ore-depositing reactions in Mississippi Valley-type deposits, *in* Kisvarsanyi, G., Grant, S.K., Pratt, W.P., and Koenig, J.W. eds., International Conference on Mississippi Valley Type Lead-Zinc Deposits: Proceedings volume: Rolla, Missouri, University of Missouri-Rolla, p. 77–85.

Barrie, C.D., Boyce, A.J., Boyle, A.P., Williams, P.J., Blake, K., Wilkinson, J.J., Lowther, M., McDermott, P., and Prior, D.J., 2009, On the growth of colloform textures: A case study of sphalerite from the Galmoy orebody, Ireland: Journal of the Geological Society, London, v. 166, p. 563–582, doi: 10.1144/0016-76492008-080.

Bastesen, E., and Rotevatn, A., 2012, Evolution and structural style of relay zones in layered limestone-shale sequences: Insights from the Hammam Faraun fault block, Suez rift, Egypt: Journal of the Geological Society, London, v. 169, p. 477–488, doi: 10.1144/0016-76492011-100.

Blakeman, R.J., Ashton, J.H., Boyce, A.J., Fallick, A.E., and Russell, M.J., 2002, Timing and interplay between hydrothermal and surface fluid in the Navan Zn + Pb orebody, Ireland: Evidence from metal distribution trends, mineral textures, and $\delta^{34}S$ analyses: Economic Geology, v. 97, p. 73–91.

Bonson, C.G., Childs, C., Walsh, J.J., Schöpfer, M.P.J., and Carboni, V., 2007, Geometric and kinematic controls on the internal structure of a large normal fault in massive limestones: The Maghlaq fault, Malta: Journal of Structural Geology, v. 29, p. 336–354, doi: 10.1016/j.jsg.2006.06.016.

Bonson, C.G., Walsh, J.J., and Carboni, V., 2012, The role of faults in localising mineral deposits in the Irish Zn-Pb orefield: Structural Geology and Resources 2012, Australian Institute of Geologists (AIG), Kalgoorlie, September 2012, Proceedings, p. 8–11.

Carboni, V., Walsh, J., Stewart, D., and Güven, J., 2003, Timing and geometry of normal faults and associated structures at the Lisheen Zn/Pb deposit—investigating their role in the transport and the trapping of metals, *in* Eliopoulos, D.G., et al., eds., Proceedings of the Seventh Biennial SGA Meeting, Mineral Exploration and Sustainable Development: Rotterdam, Millpress Science Publishers, p. 665–668.

Caumon, G., Collon-Drouaillet, P., Le Carlier de Veslud, C., Viseur, S., and Sausse, J., 2009, Surface-based 3-D modeling of geological structures: Mathematical Geosciences, v. 41, p. 927–945, doi: 10.1007/s11004-009-9244-2.

Childs, C., Watterson, J., and Walsh, J.J., 1995, Fault overlap zones within developing normal fault systems: Geological Society, London, Special Publications, v. 152, p. 535–549.

Claypool, G.E., Holser, W.T., Kaplan, I.R., Sakai, H., and Zak, I., 1980, The age curves of sulfur and oxygen isotopes in marine sulfate and their mutual interpretation: Chemical Geology, v. 28, p. 199–260.

Coller, D.W., 1984, Variscan structures in the Upper Palaeozoic rocks of west central Ireland: Geological Society, London, Special Publications, v. 14, p. 185–194, doi: 10.1144/GSL.SP.1984.014.01.18.

Cooke, D.R., Bull, S.W., Large, R.R., and McGoldrick, P.J., 2000, The importance of oxidized brines for the formation of Australian Proterozoic stratiform sediment-hosted Pb-Zn (sedex) deposits: Economic Geology, v. 95, p. 1–18.

Coomer, P.G., and Robinson, B.W., 1976, Sulphur and sulphate-oxygen isotopes and the origin of the Silvermines deposits, Ireland: Mineralium Deposita, v. 11, p. 155–169, doi: 10.1007/BF00204478.

Cooper, M.R., Anderson, H., Walsh, J.J., Van Dam, C.L., Young, M.E., Earls, G., and Walker, A., 2012, Palaeogene Alpine tectonics and Icelandic plume-related magmatism and deformation in Northern Ireland: Journal of the Geological Society, London, v. 169, p. 29–36, doi: 10.1144/0016-76492010-182.

Corbella, M., Ayora, C., and Cardellach, E., 2004, Hydrothermal mixing, carbonate dissolution, and sulfide precipitation in Mississippi Valley-type deposits: Mineralium Deposita, v. 39, p. 344–357, doi: 10.1007/s00126-004-0412-5.

Corbella, M., Ayora, C., Cardellach, E., and Soler, A., 2006, Reactive transport modeling and hydrothermal karst genesis: The example of the Rocabruna barite deposit (eastern Pyrenees): Chemical Geology, v. 233, p. 113–125, doi: 10.1016/j.chemgeo.2006.02.022.

Corbella, M., Gomez-Rivas, E., Martín-Martín, J.D., Stafford, S.L., Teixell, A., Griera, A., Travé, A., Cardellach, E., and Salas, R., 2014, Insights to controls on dolomitization by means of reactive transport models applied to the Benicàssim case study (Maestrat basin, eastern Spain): Petroleum Geoscience, v. 20, p. 41–54, doi: 10.1144/petgeo2012-095.

Cox, S.F., 2005, Coupling between deformation, fluid pressures, and fluid flow in ore-producing hydrothermal systems at depth in the crust: Economic Geology 100th Anniversary Volume, p. 39–75.

Cox, S.F., Knackstedt, M.A., and Braun, J., 2001, Principles of structural control on permeability and fluid flow in hydrothermal systems: Reviews in Economic Geology, v. 14, p. 1–24.

Cruise, M.D., 2000, Iron oxide and associated base metal mineralization in the Central Midlands basin, Ireland: Unpublished Ph.D. thesis, Dublin, Ireland, University of Dublin, 651 p.

Davidheiser-Kroll, B., 2014, Understanding the fluid pathways that control the Navan orebody: Unpublished Ph.D. thesis, Glasgow, Scotland, University of Glasgow, 233 p.

Davidheiser-Kroll, B., Boyce, A., Ashton, J., Blakeman, R., and Geraghty, J., 2013, How did it get there? Searching for "the feeder" at the Navan Zn + Pb deposit, Ireland: Mineral Deposit Research for a High-Tech World, Society for Geology Applied to Mineral Deposits (SGA), Biennial Meeting, 12th, Uppsala, Sweden, August 2013, Proceedings, p. 1–4.

Doran, A.L., Menuge, J., Hollis, S.P., Güven, J., and Dennis, P., 2017, Enhancing understanding of Irish Zn-Pb mineralization: A closer look at the Island Pod orebody, Lisheen deposit: Mineral Resources to Discover, Society for Geology Applied to Mineral Deposits (SGS), Biennial Meeting, 14th, Quebéc City, Canada, August 20–23, 2017, Proceedings, p. 597–600.

Everett, C.E., Wilkinson, J.J., and Rye, D.M., 1999, Fracture-controlled fluid flow in the Lower Palaeozoic basement rocks of Ireland: Implications for the genesis of Irish-type Zn-Pb deposits: Geological Society, London, Special Publications, v. 155, p. 247–276, doi: 10.1016/j.aqpro.2013.07.003.

Downloaded from https://pubs.geoscienceworld.org/segweb/economicgeology/article-pdf/113/7/1455/4558470/1455-1477.pdf
by Univ College Dublin user

Eyre, S.L., 1998, Geochemistry of dolomitization and Zn-Pb mineralization in the Rathdowney trend, Ireland: Ph.D. thesis, London, University of London, 419 p.

Fachri, M., Rotevatn, A., and Tveranger, J., 2013, Fluid flow in relay zones revisited: Towards an improved representation of small-scale structural heterogeneities in flow models: Marine and Petroleum Geology, v. 46, p. 144–164, doi: 10.1016/j.marpetgeo.2013.05.016.

Fallick, A.E., Ashton, J.H., Boyce, A.J., Ellam, R.M., and Russell, M.J., 2001, Bacteria were responsible for the magnitude of the world-class hydrothermal base metal sulfide orebody at Navan, Ireland: Economic Geology, v. 96, p. 885–890, doi: 10.2113/gsecongeo.96.4.885.

Faulkner, D.R., Jackson, C.A.L., Lunn, R.J., Schlische, R.W., Shipton, Z.K., Wibberley, C.A.J., and Withjack, M.O., 2010, A review of recent developments concerning the structure, mechanics and fluid flow properties of fault zones: Journal of Structural Geology, v. 32, p. 1557–1575, doi: 10.1016/j.jsg.2010.06.009.

Ferrill, D.A., and Morris, A.P., 2001, Displacement gradient and deformation in normal fault systems: Journal of Structural Geology, v. 23, p. 619–638, doi: 10.1016/S0191-8141(00)00139-5.

Fossen, H., and Rotevatn, A., 2016, Fault linkage and relay structures in extensional settings-a review: Earth-Science Reviews, v. 154, p. 14–28, doi: 10.1016/j.earscirev.2015.11.014.

Fusciardi, L.P., Güven, J.F., Stewart, D.R.A., Carboni, V., and Walsh, J.J., 2004, The geology and genesis of the Lisheen Zn-Pb deposit, Co. Tipperary, Ireland, *in* Kelly, J.G., Andrew, C.J., Ashton, J.H., Boland, M.B., Earls, G., Fusciardi, L., and Stanley, G., eds., Europe's major base metal deposits: Special Publication of the Irish Association for Economic Geology, p. 455–481.

Gagnevin, D., Boyce, A.J., Barrie, C.D., Menuge, J.F., and Blakeman, R.J., 2012, Zn, Fe, and S isotope fractionation in a large hydrothermal system: Geochimica et Cosmochimica Acta, v. 88, p. 183–198, doi: 10.1016/j.gca.2012.04.031.

Gagnevin, D., Menuge, J.F., Kronz, A., Barrie, C., and Boyce, A.J., 2014, Minor elements in layered sphalerite as a record of fluid origin, mixing, and crystallization in the Navan Zn-Pb ore deposit, Ireland: Economic Geology, v. 109, p. 1513–1528, doi: 10.2113/econgeo.109.6.1513.

Gleeson, S.A., and Yardley, B.W.D., 2002, Extensional veins and Pb-Zn mineralisation in basement rocks: The role of penetration of formation brines, *in* Stober, I., and Bucher, K., eds., Water-rock interaction: Netherlands, Kluwer Academic Publishers, p. 189–205.

Goodfellow, W., and Lydon, J., 2007, Sedimentary exhalative (SEDEX) deposits. Mineral deposits of Canada: Geological Association of Canada, Mineral Deposits Division, Special Publication 5, p. 163–183.

Goodfellow, W., Lydon, J., and Turner, R., 1993, Geology and genesis of stratiform sediment-hosted (SEDEX) zinc-lead-silver sulphide deposits: Mineral deposit modeling: Geological Association of Canada Special Paper 40, p. 201–251.

Hitzman, M.W., 1999, Extensional faults that localize Irish syndiagenetic Zn-Pb deposits and their reactivation during Variscan compression: Geological Society, London, Special Publications, v. 155, p. 233–245, doi: 10.1144/GSL.SP.1999.155.01.17.

Hitzman, M., and Beaty, D., 1996, The Irish Zn-Pb-(Ba) orefield: Society of Economic Geologists, Special Publication 4, p. 112–143.

Hitzman, M.W., and Large, R., 1986, A review and classification of the Irish carbonate-hosted base metal deposits, *in* Andrew, C.J., Crowe, R.W.A., Finlay, S., Pennell, W.M., and Pyne, J., eds., Geology and genesis of mineral deposits in Ireland: Dublin, Irish Association for Economic Geology, p. 218–238.

Hitzman, M.W., Allan, J.R., and Beaty, D.W., 1998, Regional dolomitization of the Waulsortian limestone in southeastern Ireland: Evidence of larger-scale fluid flow driven by the Hercynian orogeny: Geology, v. 26, p. 547–550.

Hitzman, M.W., Redmond, P.B., and Beaty, D.W., 2002, The carbonate-hosted Lisheen Zn-Pb-Ag deposits, County Tipperary, Ireland: Economic Geology, v. 97, p. 1627–1655, doi: 10.1126/science.289.5479.551.

Hollis, S.P., Menuge, J., Dennis, P., Güven, J.F., Boyce, A.J., and Roberts, S., 2016, Constraining fluid mixing processes at the Irish-type Lisheen and Navan Zn-Pb orebodies: Preliminary evidence from clumped C-O isotopes: 27th International Geological Congress, Cape Town, South Africa, August 27-September 4, 2016, Proceedings, p. 1–4.

Johnston, J.D., 1999, Regional fluid flow and the genesis of Irish Carboniferous base metal deposits: Mineralium Deposita, v. 34, p. 571–598, doi: 10.1007/s001260050221.

Johnston, J.D., Coller, D., Millar, G., and Critchley, M.F., 1996, Basement structural controls on Carboniferous-hosted base metal mineral deposits in Ireland: Geological Society, London, Special Publication, v. 107, p. 1–21.

Kinnaird, J.A., Ixer, R.A., Barreiro, B., and Nex, P.A., 2002, Contrasting sources for lead in Cu-polymetallic and Zn-Pb mineralisation in Ireland: Constraints from lead isotopes: Mineralium Deposita, v. 37, p. 495–511, doi: 10.1007/s00126-001-0252-5.

Kucha, H., 1989, Macrotextures, microtextures, and carbonate-sulfide relationships in stratiform, carbonate-hosted Zn-Pb orebodies of Silvermines, Ireland: Mineralium Deposita, v. 24, p. 48–55, doi: 10.1007/BF00206723.

Kyne R., Torremans K., Doyle R., Güven, J., and Walsh, J.J., 2017, Segmented fault arrays and their control on the formation of Irish-type Zn-Pb deposits: Biennial Meeting of the Society for Geology Applied to Mineral Deposits, Quebec, Canada, August 20–23, 2017, Extended Abstracts, p. 617–620.

Large, R., Bull, S., McGoldrick, P., and Walters, S., 2005, Stratiform and strata-bound Zn-Pb-Ag deposits in Proterozoic sedimentary basins, northern Australia: Economic Geology 100th Anniversary Volume, p. 931–963.

Leach, D.L., Taylor, R.D., Fey, D.L., Diehl, S.F., and Saltus, R., 2010, A deposit model for Mississippi Valley-type lead-zinc ores: U.S. Geological Survey Scientific Investigations Report 2010-5070-A, p. 1–52.

Lee, M.J., and Wilkinson, J.J., 2002, Cementation, hydrothermal alteration, and Zn-Pb mineralization of carbonate breccias in the Irish Midlands: Textural evidence from the Cooleen zone, near Silvermines, County Tipperary: Economic Geology, v. 97, p. 653–662, doi: 10.2113/gsecongeo.97.3.653.

Lowther, J., Balding, A., McEvoy, F., and Dunphy, S., 2003, The Galmoy Zn-Pb orebodies: Structure and metal distribution—clues to the genesis of the deposits, in, Fusciardi, L., Earls, G., Stanley, G., Kelly, J., Ashton, J., Boland, M., and Andrew, C.J, eds., Europe's major base metal deposits: Special Publication of the Irish Association for Economic Geology, p. 437–452.

Muchez, P., Heijlen, W., Banks, D.A., Blundell, D.J., Boni, M., and Grandia, F., 2005, Extensional tectonics and the timing and formation of basin-hosted deposits in Europe: Ore Geology Reviews, v. 27, p. 241–267, doi: 10.1016/j.oregeorev.2005.07.013.

Mullane, M.M., and Kinnaird, J.A., 1998, Synsedimentary mineralization at Ballynoe barite deposit, near Silvermines, Co. Tipperary, Ireland: Transactions of the Institution of Mining and Metallurgy, Section B: Applied Earth Science, v. 107, p. 48–61.

Philcox, M.E., 1984, Lower Carboniferous lithostratigraphy of the Irish Midlands: Dublin, Irish Association for Economic Geology, 89 p.

Philips, W.E.A., and Sevastopulo, G.D., 1986, Stratigraphic and structural setting of Irish mineral deposits, *in* Andrew, C.J., Crowe, R.W.A., Finlay, S., Pennel, W.M., and Pyne, J.F., eds., Geology and genesis of mineral deposits in Ireland: Dublin, Irish Association for Economic Geology, p. 1–30.

Redmond, P.B., 1997, Structurally controlled mineralization and hydrothermal dolomitization at the Lisheen Zn-Pb-Ag deposit, County Tipperary, Ireland: Dublin, University College Dublin, 126 p.

Reed, C.P., and Wallace, M.W., 2004, Zn-Pb mineralisation in the Silvermines district, Ireland: A product of burial diagenesis: Mineralium Deposita, v. 39, p. 87–102, doi: 10.1007/s00126-003-0384-x.

Rhoden, H.N., 1959, Mineralogy of the Silvermines district, County Tipperary, Eire: Mineralogical Magazine, v. 32, p. 128–139.

Rotevatn, A., and Bastesen, E., 2012, Fault linkage and damage zone architecture in tight carbonate rocks in the Suez rift (Egypt): Implications for permeability structure along segmented normal faults: Geological Society, London, Special Publications, v. 374, p. 79–95, doi: 10.1144/SP374.12.

Rotevatn, A., Fossen, H., Hesthammer, J., Aas, T.E., and Howell, J.A., 2007, Are relay ramps conduits for fluid flow? Structural analysis of a relay ramp in Arches National Park, Utah: Geological Society, London, Special Publications, v. 270, p. 55–71, doi: 10.1144/GSL.SP.2007.270.01.04.

Samson, I.M., and Russell, M.J., 1987, Genesis of the Silvermines zinc-lead-barite deposit, Ireland; fluid inclusion and stable isotope evidence: Economic Geology, v. 82, p. 371–394, doi: 10.2113/gsecongeo.82.2.371.

Sevastopulo, G.D., and Redmond, P., 1999, Age of mineralization of carbonate-hosted, base metal deposits in the Rathdowney trend, Ireland: Geological Society, London, Special Publications, v. 155, p. 303–311, doi: 10.1144/GSL.SP.1999.155.01.20.

Sevastopulo, G.D., and Wyse Jackson, P.N., 2009, Carboniferous: Mississippian (Tournasisian and Viséan), *in* Holland, C.H., and Sanders, I.S, eds., The geology of Ireland, 2nd ed.: Edinburgh, Dunedin Academic Press, p. 215–268.

Shearley, E., Redmond, P.B., King, M., and Goodman, R., 1996, Geological controls on mineralization and dolomitization of the Lisheen Zn-Pb-Ag

Downloaded from https://pubs.geoscienceworld.org/segweb/economicgeology/article-pdf/113/7/1455/4558470/1455-1477.pdf
by Univ College Dublin user

deposit, Co. Tipperary, Ireland: Geological Society, London, Special Publications, v. 107, p. 23–33.
Stewart, D.R.A., 1999, The occurrence, characterization, and genesis of melanterite at Lisheen mine, Co. Tipperary, Ireland: Unpublished M.Sc. thesis, Leicester, University of Leicester, 35 p.
Strogen, P., Jones, G.L., and Somerville, I.D., 1990, Stratigraphy and sedimentology of Lower Carboniferous (Dinantian) boreholes from West Co. Meath, Ireland: Geological Journal, v. 25, p. 103–137.
Sverjensky, D.A., 1986, Genesis of Mississippi Valley-type lead-zinc desposits: Annual Review of Earth and Planetary Sciences, v. 14, p. 177–199, doi: 10.1146/annurev.ea.14.050186.001141.
Taylor, S., 1984, Structural and paleotopographic controls of lead-zinc mineralization in the Silvermines orebodies, Republic of Ireland: Economic Geology, v. 79, p. 529–548, doi: 10.2113/gsecongeo.79.3.529.
Taylor, S., and Andrew, C., 1978, Silvermines orebodies, County Tipperary, Ireland: Transactions of the Institution of Mining and Metallurgy, Section B: Applied Earth Science, v. 87, p. B111–B124.
Turner, O., and McClenaghan, S.H., 2017, Trace-element variation in pyrites within the Derryville ore body, Lisheen mine, Ireland: Mineral Resources to Discover, Society for Geology Applied to Mineral Deposits (SGS), Biennial Meeting, 14th, Quebéc City, Canada, August 20–23, 2017, Proceedings, p. 689–692.
Walsh, J.J., and Watterson, J., 1988, Analysis of the relationship between displacements and dimensions of faults: Journal of Structural Geology, v. 10, p. 239–247.
Walsh, J.J., Watterson, J., Bailey, W.R., and Childs, C., 1999, Fault relays, bends, and branch-lines: Journal of Structural Geology, v. 21, p. 1019–1026, doi: 10.1016/S0191-8141(99)00026-7.
Walsh, J.J., Bailey, W.R., Childs, C., Nicol, A., and Bonson, C.G., 2003, Formation of segmented normal faults: A 3-D perspective: Journal of Structural Geology, v. 25, p. 1251–1262, doi: 10.1016/S0191-8141(02)00161-X.
Walshaw, R.D., Menuge, J.F., and Tyrrell, S., 2006, Metal sources of the Navan carbonate-hosted base metal deposit, Ireland: Nd and Sr isotope evidence for deep hydrothermal convection: Mineralium Deposita, v. 41, p. 803–819, doi: 10.1007/s00126-006-0100-8.
Wilkinson, J.J., 2010, A review of fluid inclusion constraints on mineralization in the Irish ore field and implications for the genesis of sediment-hosted Zn-Pb deposits: Economic Geology, v. 105, p. 417–442, doi: 10.2113/gsecongeo.105.2.417.
——2014, Sediment-hosted zinc-lead mineralization, *in* Holland, H., and Turekian, K., eds., Treatise on Geochemistry, v. 13: Elsevier, p. 219–249.
Wilkinson, J.J., Everett, C.E., Boyce, A.J., Gleeson, S.A., and Rye, D.M., 2005a, Intracratonic crustal seawater circulation and the genesis of subseafloor zinc-lead mineralization in the Irish orefield: Geology, v. 33, p. 805–808, doi: 10.1130/G21740.1.
Wilkinson, J.J., Eyre, S.L., and Boyce, A.J., 2005b, Ore-forming processes in Irish-type carbonate-hosted Zn-Pb deposits: Evidence from mineralogy, chemistry, and isotopic composition of sulfides at the Lisheen Mine: Economic Geology, v. 100, p. 63–86, doi: 10.2113/100.1.0063.
Wilkinson, J.J., Stoffell, B., Wilkinson, C.C., Jeffries, T.E., and Appold, M.S., 2009, Anomalously metal-rich fluids form hydrothermal ore deposits: Science, v. 323, p. 764–767, doi: 10.1126/science.1164436.
Wilkinson, J.J., Crowther, H.L., and Coles, B.J., 2011, Chemical mass transfer during hydrothermal alteration of carbonates: Controls of seafloor subsidence, sedimentation, and Zn–Pb mineralization in the Irish Carboniferous: Chemical Geology, v. 289, p. 55–75, doi: 10.1016/j.chemgeo.2011.07.008.
Worthington, R.P., and Walsh, J.J., 2011, Structure of Lower Carboniferous basins of NW Ireland, and its implications for structural inheritance and Cenozoic faulting: Journal of Structural Geology, v. 33, p. 1285–1299, doi: 10.1016/j.jsg.2011.05.001.
Yardley, B.W.D., 2005, 100th anniversary special paper: Metal concentrations in crustal fluids and their relationship to ore formation: Economic Geology, v. 100, p. 613–632, doi: 10.2113/gsecongeo.100.4.613.

Koen Torremans is a structural geologist who specializes in mineral deposits in sedimentary basins. He is currently a Marie Skłodowska-Curie postdoctoral fellow based at iCRAG, the Irish Centre for Research in Applied Geosciences in University College Dublin, Ireland. Koen received his B.Sc., M.Sc., and Ph.D. (2016) degrees from KU Leuven University in Belgium. He has worked extensively on base metal deposits in the Central African Copperbelt and the Irish ore field, applying a wide variety of techniques to elucidate ore deposit formation, fluid flow, and structural controls. This includes structural analysis, basin analysis, geochemistry, and geologic and numerical modeling techniques.

Downloaded from https://pubs.geoscienceworld.org/segweb/economicgeology/article-pdf/113/7/1455/4558470/1455-1477.pdf
by Univ College Dublin user

Downloaded from https://pubs.geoscienceworld.org/segweb/economicgeology/article-pdf/113/7/1455/4558470/1455-1477.pdf
by Univ College Dublin user